Burkholderia Genes Involved in Extracellular Bioplastic Degradation Revealed by Tn-seq and CRISPR-Cas

Running title: Extracellular Bioplastic Degradation in *Burkholderia* by Tn-seq and CRISPR-Cas

Zhong Ling Yap[a], Gabriel G. Lucas[b], Mohamad Safklou[a], Ryan Darragh[a], Andrew M. Hogan[a], Anna Motnenko[a], Warren Blunt[c], Richard Sparling[a], David B. Levin[c], Dario Fernández Do Porto[b], Silvia T. Cardona[a,d*]

[a]Department of Microbiology, University of Manitoba, Winnipeg, Manitoba, Canada R3T 2N2

[b]Plataforma de Bioinformática Argentina, Instituto de Cálculo, Ciudad Universitaria, Facultad de Ciencias Exactas y Naturales, Universidad de Buenos Aires (UBA), Ciudad Autónoma de Buenos Aires, Argentina

[c]Department of Biosystems Engineering, University of Manitoba, Winnipeg, Manitoba, Canada R3T 5V6

[d]Department of Medical Microbiology and Infectious Diseases, University of Manitoba, Winnipeg, Manitoba, Canada R3E 0J9

email: silvia.cardona@umanitoba.ca

Keywords: *Burkholderia*, *Burkholderia vietnamiensis*, Transposon mutagenesis, CAST, gene insertion

Abstract

Bioplastics represent promising alternatives to petroleum-based plastics, yet their biodegradation remains insufficiently understood. Identifying bacteria capable of degrading bioplastics extracellularly could enhance end-of-life management practices. To investigate *Burkholderia*'s capacities for the degradation of medium-chain-length polyhydroxyalkanoate (mcl-PHA), we screened a panel of *Burkholderia* strains and identified such capacity in some strains of *B. gladioli*, *B. multivorans,* and *B. vietnamiensis*. To elucidate the genetic basis of this activity, we performed transposon mutagenesis followed by activity-based screening and Tn-seq on *B. vietnamiensis* LMG 16232. Transposon insertions with negative phenotype were identified in genes encoding a triacylglycerol lipase, a lipase chaperone, type II secretion system components, HTH-type transcriptional activators, and a polyhydroxyalkanoate synthesis repressor. To validate the involvement of these genetic elements in mcl-PHA degradation, we generated insertional mutants using a CRISPR-associated transposase system (CAST). Complete loss or reduced extracellular mcl-PHA depolymerase activity was observed in the CAST mutants, validating their involvement in mcl-PHA degradation. In addition, the interruption of these genetic elements showed a loss of lipase activity, suggesting that the enzymes responsible for mcl-PHA depolymerase are lipases with substrate ambiguity; moreover, docking experiments supported these findings. Together, we identify *B. vietnamiensis* as a source of enzymes capable of degrading extracellular mcl-PHA and demonstrate the power of combining activity-based screening, Tn-seq, and CAST to rapidly establish gene-to-function links.

41 **Importance**

42 Due to their versatile metabolism, *Burkholderia* strains play critical roles in degradation of
43 multiple compounds in the environment. Here we show that several Burkholderia species can
44 degrade medium-chain-length polyhydroxyalkanoates (mcl-PHAs), a promising class of
45 bioplastics. By integrating transposon mutagenesis, Tn-seq, and CRISPR-associated transposase
46 (CAST) technologies, we identify and validate key genetic determinants involved in mcl-PHA
47 degradation in B. vietnamiensis. These genes encode a lipase, a secretion system component, and
48 regulatory factors, underscoring the complexity and specificity of microbial bioplastic degradation
49 pathways. The findings not only advance our understanding of PHA biodegradation but also
50 identifies *B. vietnamiensis* as as a source of enzymes capable of degrading extracellular mcl-PHA.
51

52 **Introduction**

53 Environmental pollution from petroleum-based plastic has driven growing interest in
54 bioplastics, which are bio-based, biodegradable substitutes. Among these, poly(3-
55 hydroxyalkanoates) (PHAs) are biologically produced polyesters that have a wide-range of
56 applications in various sectors, such as packaging, agriculture, and biomedical devices (1). PHAs
57 are synthesized by many microorganisms for intracellular energy and carbon storage under
58 conditions of nutrient imbalance, namely nitrogen and phosphorous limitation. Depending on the
59 number of carbon atoms in each 3-hydroxyalkanoate monomer unit, PHAs can be broadly
60 classified as either short-chain-length PHAs (scl-PHA), which consist of 3–5 carbons per monomer
61 or medium-chain-length PHAs (mcl-PHA), which contain, 6–14 carbons per monomer, each with
62 different physico-chemical properties (2). The monomer of the carbon side chain length of PHAs
63 will influence the enzyme-substrate specificity for degradation (3).

64 PHAs are degraded by either intracellular or extracellular PHA depolymerases.
65 Intracellular PHA depolymerases hydrolyze PHA located in carbonosomes, which are endogenous
66 carbon reservoirs or in native amorphous PHA granules, which have a surface layer of proteins
67 and phospholipids (4). Extracellular PHA depolymerases degrade exogenous denatured granules
68 that are semi-crystalline and lack the surface layer (3). Both intracellular and extracellular PHA
69 depolymerases are carboxylesterases and belong to the α/β-hydrolase fold family (5). PHA
70 depolymerases have been isolated and biochemically characterized in Ascomycetes, Firmicutes,
71 Proteobacteria, and Actinobacteria (6).

72 Many studies have reported microorganisms that degrade scl-PHA and have purified, and
73 characterized the corresponding enzymes (5, 6). However, microorganisms that can degrade mcl-
74 PHA are relatively rare compared to those that can degrade scl-PHA (6). Most of the extracellular

75 mcl-PHA depolymerases that have been purified and biochemically validated belong to
76 *Pseudomonas* sp. (7–9), the obligated predator *Bdellovibrio bacteriovorus* (10), *Thermus*
77 *thermophilus* (11) and the Actinobacteria *Streptomyces* sp (12–14). Amino acid sequence
78 similarity searches of metagenomes using biochemically validated extracellular mcl-PHA
79 depolymerases as queries, have identified candidate extracellular mcl-PHA depolymerases only in
80 the taxonomic groups Myxococcota, Proteobacteria, Actinobacteriota and Bdellovibrionota (6).
81 These studies suggest that mcl-PHA degradation is not widely distributed among Bacteria.

82 While all extracellular PHA depolymerases hydrolyze PHA, extracellular mcl-PHA
83 depolymerases show little overall sequence homology with scl-PHA despite both being involved
84 in the degradation of PHAs. However, most PHA depolymerases share structural and mechanistic
85 characteristics with lipases and other α/β-hydrolase enzymes (15). Both PHA depolymerases and
86 lipases have a catalytic triad consisting of serine, histidine, and aspartic acid at the active site. The
87 catalytic serine is located within the GxSxG sequence motive (also known as lipase box), also
88 found in other α/β-hydrolases. Furthermore, a conserved non-catalytic histidine near the oxyanion
89 hole is positioned and functions similarly to the corresponding residue in lipases (3, 5, 16),
90 underscoring putative functional promiscuity between PHA depolymerases and lipases. Indeed,
91 extracellular lipases were purified from various species, including *Bacillus subtilis, Pseudomonas*
92 *aeruginosa, Pseudomonas alcaligenes,* and *Pseudomonas fluorescens* (16). However, most of
93 these lipases were not able to hydrolyze poly3-hydroxyhexanoate or poly3-hydroxybutyrate.
94 While the extracellular lipases of *Pseudomonas chlororaphis* PA23 and *Acinetobacter lwoffii* can
95 hydrolyze various PHA polymers, including mcl-PHA: polyhydroxyoctanoate (PHO) and
96 polyhydroxydecanoate (17), it is not known if *Burkholderia* strains, which are known lipase
97 producers (18–21) possess the capacity to degrade extracellular mcl-PHA.

98 In this work, we used poly(3-hydroxyoctanoate) (PHO) to explore extracellular mcl-PHA
99 degradation in *B. vietnamiensis* LMG 16232 and identified the genetic elements involved in this
100 process. Transposon mutagenesis followed by activity-based screening and Tn-seq identification
101 of transposon insertions linked genes with loss of extracellular mcl-PHA degradation. The
102 identified genes encode a putative triacylglycerol lipase, a lipase chaperone, type II secretion
103 system components, an HTH-type transcriptional activator, and a polyhydroxyalkanoate synthesis
104 repressor. By combining activity-based screening with the power of random and site-directed
105 transposon mutagenesis to rapidly identify all genetic elements that contribute to a specific
106 function, we were able to uncover genes associated mcl-PHA degradation that would not have
107 been predicted based on gene annotation.

108 **Results**

109 *Diversity of extracellular mcl-PHA degradation activity in Burkholderia strains*

110 To identify mcl-PHA degradation activity in the *Burkholderia* genus, we performed an
111 initial screen in a solid minimal medium containing PHO and limiting amounts of phenylalanine,
112 supplemented with Nile red to enhance the visualization of PHO degradation as a clear halo around
113 isolated bacterial colonies. Phenylalanine was chosen as a secondary carbon source in the medium
114 because (i) it is known to be catabolized by *Burkholderia* species (22), and (ii) its metabolism is
115 known to influence several bacterial pathways (23). The plates were incubated for 20 days to
116 ensure cells grew densely and produced sufficient enzyme to visually detect mcl-PHA degradation.
117 After dense growth was achieved, a clear halo was observed around some colonies, suggesting
118 extracellular PHO degradation.

119 Several strains of *B. gladioli*, *B. multivorans*, and *B. vietnamiensis,* were able to produce a
120 visible halo suggesting extracellular mcl-PHA degradation (**Table 1, Fig. S1**). Of the strains with

activity, *B. gladioli* strain VC19233, *B. multivorans* 21NH942533, and VC9825 exhibited weak activity in degrading mcl-PHA; *B. stagnalis* strains MSMB618, MSMB642, and *B. vietnamiensis* LMG 16232 had moderate activity in degrading mcl-PHA. There were two strains, *B. multivorans* F9091687 and *B. gladioli* 132208, where the temperature affected the activity. No mcl-PHA depolymerase activity was observed for *B. cenocepacia*, *B. contaminans,* and *B. dolosa* isolates tested (**Table 1**).

Genetic basis of B. vietnamiensis LMG 16232 extracellular mcl-PHA degradation activity

To determine the gene elements involved in the extracellular mcl-PHA degradation activity we chose *B. vietnamiensis* LMG 16232 as ongoing work in our lab suggested its genetic manipulation amenability by a ShCAST-based genetic tool for targeted insertional mutagenesis (24). After sequencing its genome (25) we performed transposon mutagenesis and activity-based screening followed by identification of transposon sites with Illumina sequencing (Tn-seq) (**Fig. 1**). To achieve genomic coverage of transposon insertions in *B. vietnamiensis* LMG 16232, we determined the estimated transposon insertion density using an analytical model based on a Poisson distribution of transposon insertions (26) (see material and methods).

The primary screening of single isolated transconjugants identified 84 colonies that did not produce a visible halo. These colonies were subjected to secondary screening, where each isolated transconjugant clone was propagated and screened on solid medium containing mcl-PHA. We observed that 66 transconjugants had lost the ability to degrade extracellular mcl-PHA, showing no halo (Pool 1). In contrast, 18 transconjugants exhibited a reduced halo (Pool 2). The complete list of transposon mutants from pool 1 and pool 2 are shown in Table 2.

Further examination of the putative functions of the genes identified by transposon insertions identified a gene cluster that encodes a type II secretion system (**Fig. 2A**), and a lipase

144 gene cluster, encoding triacylglycerol lipases, (designated as *lip1* and *lip2* herein) and a lipase
145 chaperone, (designated as *lipO*) (**Fig. 2B**). Additionally, three transposons mapped to a *pha* gene
146 cluster. Transposons in this cluster were found in *phaR* (P4G95_13560), a polyhydroxyalkanoate
147 synthesis repressor and *phaA* (P4G95_13570), which encodes for an acetyl-CoA acetyltransferase
148 involved in the biosynthesis of polyhydroxybutyrate (**Fig. 2C**). In addition, a gene coding for a
149 A24 family peptidase (P4G95_07805) and four genes encoding transcriptional regulators were
150 identified, which are a TetR/AcrR family transcriptional regulator (P4G95_00865), a MarR family
151 winged helix-turn-helix transcriptional regulator CDS (P4G95_05570), *phaR* (P4G95_13560), the
152 polyhydroxyalkanoate synthesis repressor, and a helix-turn-helix domain-containing protein CDS
153 (P4G95_16325) (Table 2). Together these results suggest that *lip1* (P4G95_16805) might be the
154 enzyme responsible for extracellular mcl-PHA degradation. The lipase encoded by *lip1* contains a
155 signal peptide probably cleaved by the A24 family peptidase (P4G95_07805). In the periplasm,
156 the lipase chaperone, *lipO* (P4G95_16815), may be responsible for folding and activating the
157 lipase prior to secretion. Finally, the lipase may be then finally excreted to extracellular space via
158 a type II secretion system (P4G95_05485, P4G95_05490, P4G95_05495, P4G95_05500,
159 P4G95_05505, P4G95_05510, P4G95_05515, P4G95_05520, P4G95_05525, P4G95_05530,
160 P4G95_05535).

161 A few genetic elements obtained from the Tn-seq analysis had a less clear relation with
162 extracellular mcl-PHA degradation in *B. vietnamiensis* LMG 16232. These were genes encoding
163 for trehalose-6-phosphate phosphatase (P4G95_10885), hypothetical proteins (P4G95_20805 and
164 P4G95_20810), the N-acetylglucosamine-6-phosphate deacetylase, NagA (P4G95_03530), a
165 phenylacetate-CoA oxygenase/reductase subunit PaaK and PaaJ (P4G95_06510 and
166 P4G95_06515) and an acetyl-CoA acetyltransferase PhaA (P4G95_13570).

167 *Characteristics of a mcl-PHA degrading enzyme in B. vietnamiensis LMG 16232 predicted via in*
168 *silico analysis*

169 Bacterial lipases are known to be capable of degrading polymers, such as polycaprolactone,
170 polyethylene terephthalate, and mcl-PHA (16, 27). The genome of *B. vietnamiensis* LMG 16232,
171 contains three genes putatively associated with lipase function: P4G95_16805 and P4G95_16810,
172 both coding for a triacylglycerol lipase, and P4G95_14150, coding for a lipase family protein.
173 While these candidate genes could encode enzymes capable for mcl-PHA degradation, our
174 activity-based screening followed by Tn-seq analysis identified that clones that have lost the halo
175 of PHO degradation, had transposon insertions in the P4G95_16805 locus (*lip1*), but not in the
176 other genes with predicted lipase activity.

177 The *lip1*-encoded protein, GenBank: WHU94860.1 is a putative triacylglycerol lipase that
178 shows common features to other extracellular lipases and mcl-PHA depolymerase, such as
179 containing a signal peptide and a catalytic triad composed of a serine (embedded in a lipase box
180 motif), histidine and aspartic acid (5). This enzyme is predicted to have 364 amino acids, with a
181 calculated molecular weight of 37.6 kDa and a theoretical isoelectric point (pI) of 6.43, computed
182 with Expasy (28). The computed molecular mass and isoelectric point are in the range of currently
183 known mcl-PHA depolymerase, where the molecular range is approximately 25 to 41 kDa, and
184 the pI value is mainly in the acidic range (11). This enzyme was predicted via SignalP 5.0 to be
185 secreted via secretory signal peptides transported by the Sec translocon and cleaved by Signal
186 Peptidase I (Lep) with a probability of 0.83. Signal peptidase I is essential in many bacteria
187 functions, and it could be the reason why insertional mutants in *LepB* (P4G95_10750) were not
188 recovered. The cleavage site position was predicted between 43-44 with a probability of 0.5069.
189 The presence of the motive (G-H-S-Q-G) in the amino acid sequence encode by *lip1* aligns with

190 the lipase box consensus sequence. This sequence has also been found in a previously identified
191 novel subgroup of extracellular mcl-PHA depolymerases from Actinobacteria, specifically those
192 from *S. roseolus* and *S. venezuelae*, and *S. exfoliates* (12–14).

193 In contrast, extracellular mcl-PHA depolymerases identified from the genus *Pseudomonas*
194 (7–9), as well as in *Bdellovibrio* (10), exhibit a different lipase consensus sequence, which is (G-
195 I-S-S-G). This putative protein sequence (WHU94860.1) shows very little sequence similarity to
196 currently known enzymes which can degrade mcl-PHA from the genus *Streptomyces*,
197 *Pseudomonas*, and *Bdellovibrio,* where there is only 9 to 12 % sequence identity (**Fig. 3**). The
198 enzyme also has a putative catalytic amino acid (Ser131-Asp308-His330). In summary, while *in*
199 *silico* analysis shows that P4G95_16805 codes for a lipase, the low similarity of this protein with
200 other mcl-PHA depolymerases makes *in silico* prediction for PHA degradation activity difficult.
201 While Tn-seq analysis strongly suggests that the activity of the encoded protein is that of an
202 extracellular mcl-PHA depolymerase, further validation is required.

203 *Genetic elements responsible for mcl-PHA degradation are confirmed by RhaCAST*

204 To validate the genetic elements involved in extracellular mcl-PHA degradation activity
205 identified by Tn-seq, we created independent insertional mutants using RhaCAST (24) and
206 investigated their phenotypes. RhaCAST is a genetic tool we recently developed for targeted
207 insertional mutagenesis in *Burkholderia cepacia* complex and previously applied on *B.*
208 *cenocepacia* and *B. multivorans.* We applied RhaCAST in *B. vietnamiensis* LMG 16232
209 interrupting the coding genes for the putative lipase (*lip1*, P4G95_16805), A24 family peptidase
210 (*A24*, P4G95_07805), the TetR/AcrR family transcriptional regulator (*tetR/acrR*, P4G95_00865),
211 trehalose-phosphatase (*otsB,* P4G95_10885), and a gene from type II secretion system (*gspE*,

212 P4G95_05530) (**Fig. S2-S6**). These mutants did not produce a halo around the mutant strain in an
213 agar plate containing mcl-PHA (**Fig. 4**).

214 To further confirm that the halo of degradation observed resulted from the putative lipase
215 is mcl-PHA degradation, a plug of agar from underneath the inoculated mutant was taken,
216 *lip1::CAST-Tp* and wild type as control from the agar-based assay. We determined the absence
217 and presence of PHO in the agar with gas chromatography with flame ionization detection (GC-
218 FID). As expected, no PHO was detected in the agar beneath the WT strain, whereas PHO was
219 detected under the *lip1*::CAST-Tp strain, indicating that PHO was not being degraded (**Fig. 5**).

220 To determine if the *B. vietnamiensis* LMG 16232 putative lipase and the genes that we
221 chose to make the insertional mutant are involved in mcl-PHA degradation are also involved in
222 lipid degradation, we tested *B. vietnamiensis* LMG 16232 and its mutants for tributyrin
223 degradation. The wild type *B. vietnamiensis* LMG 16232 exhibited high activity against tributyrin.
224 The mutant *lip1::CAST-Tp* exhibited reduced activity in degrading tributyrin, suggesting other
225 lipases or esterases might be produced and secreted. By disrupting *gspE,* which is part of the gene
226 cluster encoding for the type II secretion system, the mutant (*gspE::CAST-Tp*) showed complete
227 abrogation of tributyrin degradation, indicating that the lipases or esterases might be produced and
228 secreted via type II secretion system. Disrupting the gene encoding for A24 family peptidase also
229 completely abolishes tributyrin degradation, suggesting that the lipases or esterases responsible for
230 tributyrin degradation are extracellular enzymes with a leader peptide. For the TetR/AcrR family
231 transcriptional regulator insertional mutant, the ability to degrade tributyrin was reduced to
232 residual activity (**Fig. 6**).

233 *In silico analysis: structural properties of catalytic site and docking*

234 In the gene cluster of *lip1,* there is another lipase-encoding gene, *lip2* located adjacent to
235 *lip1* (**Fig. 2**). This lipase gene cluster comprises *lip1*, *lip2* and *lipO* (P4G95_16805, P4G95_16810,
236 and P4G95_16815). Transposon insertions located in clones with no halo of degradation that
237 mapped to this region were located in *lip1* and *lipO*, but not in the *lip2* gene, posing the question
238 of whether *lip2* codes for an active mcl-PHA depolymerase. To investigate this possibility, we
239 decided to analyze and compare the predicted structures of these proteins. To determine the
240 differences in the structural properties of the target proteins, we predicted the structures of Lip1
241 and Lip2 using AlphaFold 2 and analyzed multiple sequence alignments, AlphaFold predicted
242 structural confidence, and inter-residue error estimates. The sequence coverage analysis, which
243 combines alignment depth and sequence identity, illustrates the extent of conservation across
244 homologous sequences for both proteins (**Fig. S7A**). A well-conserved core region (residues ~50–
245 160) is evident in both cases, with lower coverage and diversity in the N- and C-terminal regions
246 suggesting flexible or functionally variable domains. To evaluate the reliability of the structural
247 predictions, we examined the Predicted Aligned Error (PAE) matrices of the five top-ranked
248 AlphaFold models (**Fig. S7B**). As expected, low predicted error values (blue) correspond to well-
249 defined domains, while higher values (red) are associated with flexible or ambiguous regions. The
250 consistent patterns observed across different models support a robust domain architecture with
251 potential inter-domain flexibility. Additionally, the predicted Local Distance Difference Test
252 (pLDDT) scores (**Fig. S7C**) further validate the confidence in structural predictions. The high
253 pLDDT values (>90) in the core region confirm a well-defined fold, whereas significant drops
254 around residues 50–100 and 200–250 suggest intrinsically disordered or flexible regions. These
255 trends are consistent across both Lip1 and Lip2, reinforcing the reliability of the predictions and
256 indicating a shared structural organization.

257 The superposition of the AlphaFold-predicted Lip1 and Lip2 (not shown) structures with
258 the 4LIP crystallographic template (**Fig. S8A**) revealed a high degree of structural similarity,
259 particularly in the conserved secondary structure elements. However, a notable difference was
260 observed in the predicted models of Lip1 and Lip2, where an alpha-helix appears to obstruct a
261 cavity present in 4LIP (**Fig. S8B**).

262 To evaluate the catalytic site and determine whether Lip1 and Lip2 possess enzymatic
263 activity, we performed a structural superposition with 4LIP. The overlay reveals a remarkable
264 similarity in the spatial arrangement of the catalytic triad (**Fig. S9**). The conserved positioning of
265 the key catalytic residues strongly suggests that Lip1 and Lip2 adopt a functional fold compatible
266 with lipase activity. This structural conservation provides additional support for the hypothesis
267 that both proteins share mechanistic features with known lipases.

268 Using 4LIP as a template, we guided the docking of LIP1 and LIP2 with two substrates: 3-
269 Hydroxyoctanoate (OCT) and Tributyrin (TRI). Both ligands, OCT and TRI, were energy-
270 minimized before docking, and a grid-based docking algorithm was used to position the ligands
271 within the predicted active sites of both proteins. Notably, all combinations of protein-ligand
272 docking yielded clusters with low energy, indicating favourable interactions (**Table S1**).

273 Docking simulations with Lip1 revealed a single predominant low-energy cluster for both
274 OCT and TRI (**Fig. 7A, B, E, Table S1**). This convergence, together with the consistently low
275 binding energies, strongly suggests a high affinity between Lip1 and both ligands. In contrast, the
276 docking of both ligands against Lip2 (**Fig. 7C, D, E, Table S1**) yielded three distinct low-energy
277 clusters for each substrate. This multiplicity of binding modes suggests a weaker or less specific
278 interaction, potentially due to a more flexible or heterogeneous binding pocket that compromises

279 optimal substrate accommodation. Structural analysis of the catalytic site revealed that Lip1 and
280 4LIP share a similar configuration, whereas Lip2 contains a different amino acid at position 73
281 compared to Lip1, which is GLN (Lip2) instead of TYR (Lip1) (**Fig. 8, Fig. S10**). This amino acid
282 difference may explain the activities observed between Lip1, which retains enzymatic function,
283 and Lip2, in which detectable activity could not be linked to the *lip1* gene by loss of function-
284 derived transposon mutagenesis.

285 **Discussion**

286 The production and use of bioplastic, including mcl-PHA, has increased recently. These
287 materials are considered alternatives to petroleum-based plastics because they can be derived from
288 renewable resources and have a wide range of applications (1). Despite growing interest,
289 microorganisms and enzymes capable of degrading mcl-PHA remain relatively understudied (6).
290 Extracellular mcl-PHA depolymerases have been found in various genera, including *Pseudomonas*
291 (7–9), *Bdellovibrio* (10), *Thermus* (11) and *Streptomyces* (12–14). However, to date, the
292 mechanism of action for extracellular mcl-PHA by microorganisms has not been thoroughly
293 explored. Here, we report that several *Burkholderia* strains, including *B. gladioli*, *B. multivorans*,
294 and *B. vietnamiensis,* can degrade mcl-PHA. Through transposon mutagenesis combined with Tn-
295 seq analysis, we identified genetic elements associated with mcl-PHA degradation in *B.*
296 *vietnamiensis* LMG 16232. We further validated some of these genetic elements by generating
297 insertional mutants using a CRISPR-associated transposase system (CAST) in extracellular mcl-
298 PHA degradation activity. Our findings indicate that the enzyme responsible for extracellular mcl-
299 PHA degradation is a lipase with substrate versatility.

300 A technique commonly used to enhance the visualization of mcl-PHA degradation involves
301 incorporating Nile red, a lipophilic fluorescent dye, into agar plates (29). Thus, we adopted this

302 visualization method in our screening medium to increase sensitivity. In comparison to other
303 studies, where the degradation of extracellular mcl-PHA can be observed within 2 to 3 days,
304 *Burkholderia vietnamiensis* LMG16232 exhibited a slower degradation process, requiring
305 approximately 7 days for observable activity. Some strains of *Burkholderia* from the initial
306 screening showed weak activity, with degradation taking up to 20 days, despite the use of Nile red
307 to enhance detection. Nevertheless, by implementing this visualization technique and alongside
308 transposon mutagenesis in *B. vietnamiensis* LMG 16232, we were able to screen 50,000 individual
309 colonies in a rapid manner. This approach enabled us to identify transconjugant colonies that had
310 lost the ability to degrade mcl-PHA, providing a sensitive and efficient screening method. This
311 method may be applicable to other polymers that can be stained with suitable dyes, enhancing
312 assay sensitivity.

313 According to the data on the PHA depolymerase engineering database, several species of
314 *Burkholderia,* including *Burkholderia thailandensis*, *Burkholderia ambifaria, Burkholderia*
315 *graminis*, *Burkholderia cenocepacia*, *Burkholderia dolosa*, *Burkholderia multivorans*, *B.*
316 *vietnamiensis* and *Burkholderia oklahomensis* have genes encoding proteins putatively capable of
317 degrading extracellular scl-PHA (5). While *B. cepacia* DP1 has been shown to degrade
318 extracellular scl-PHA (30, 31), there are no reports of *Burkholderia* species that degrade
319 extracellular mcl-PHA. We show evidence of *Burkholderia*'s capability to degrade extracellular
320 mcl-PHA, linking the enzymatic activity to the P4G95_16805 locus of *B. vietnamiensis* LMG
321 16232.

322 *Burkholderia* is a is known as a major lipase producer. Many strains can secrete
323 extracellular lipases under inducing conditions, and some of those lipases are capable of degrading
324 various compounds (32–35). For example, lipases from *Burkholderia* stains MC 16-3 (GenBank:

325 AY772173) and 99-2-1 (GenBank: AY772174) can degrade methyl(R)-N-(2,6-dimethyl-
326 phenyl)alaninate (36). Additionally, lipase from *B. cepacia* PBSA-1 (GenBank: EF189714.1) has
327 been shown to degrade poly(butylene succinate-co-butylene adipate) (37), while *B. cepacia* lipase
328 can degrade Polycaprolactone (PCL) (16). These lipases, including the one identified in this work,
329 share a conserved lipase consensus sequence of G-H-S-Q-G, resembling the oxyanion hole
330 consensus sequence. Enzymes that degrade extracellular mcl-PHA exhibit similar characteristics
331 to these extracellular lipases, including the presence of the lipase box and a conserved non-catalytic
332 histidine near the oxyanion hole (3, 5, 16). Consequently, this study suggests that the mcl-PHA
333 degrading enzyme from *Burkholderia* are lipases that also possess the capability to degrade mcl-
334 PHA.

335 Besides the identification of the gene responsible for mcl-PHA degradation activity,
336 transposon mutagenesis combined with Tn-seq identified other genetic elements involved in the
337 degradation of mcl-PHA in *B. vietnamiensis* LMG 16232. These genes can be classified into three
338 functional groups: a) lipase/chaperone gene cluster, b) components of type II secretion system, and
339 c) regulatory elements. The genetic elements associated with the mcl-PHA degradation in *B.*
340 *vietnamiensis* LMG 16232 are consistent with the findings in various *Burkholderia* lipases,
341 particularly regarding the production and secretion of extracellular lipase. It is well established
342 that *Burkholderia* extracellular lipases are secreted through the type II secretion system. In this
343 process, the N-terminal signal peptide is transported across the inner membrane via the Sec
344 secretion system. Once in the periplasm, a chaperone interacts with the lipase, facilitating the
345 formation of the active form of the lipase (38, 39). This work also supports that the extracellular
346 lipase of *Burkholderia* depends on a dedicated chaperone. In *B. glumae*, this chaperone (lipase-
347 specific foldase) facilitates lipase folding, functioning similarly to the propeptide domains found

348 in bacterial proteases (39). Similar to the lipases in *B. cepacia* and *B. glumae*, the putative lipase
349 responsible for degrading mcl-PHA from *B. vietnamiensis* LMG 16232 is predicted to have an N-
350 terminal signal peptide. In addition, the gene encoding a chaperone is located downstream of the
351 putative lipase gene and is predicted to assist the correct folding and efficient secretion of this
352 putative lipase (40, 41). This putative enzyme (WHU94860.1), encoded by *lip1,* is likely secreted
353 via the general secretion pathway (GSP), also known as the type II secretion system, which relies
354 on a signal sequence for translocation. This mechanism is similarly predicted for the excretion of
355 the enzyme that degrades extracellular mcl-PHA in *B. bacteriovorus* (10).

356 One of the putative regulatory elements identified in this work is a TetR/AcrR family
357 transcriptional regulator CDS (P4G95_00865). This type of regulator is widely distributed among
358 bacteria and controls various cellular processes, including the metabolism of lipid compounds,
359 such as the synthesis and degradation of fatty acid and the storage of polymer (42). The
360 involvement of other regulatory elements, such as HTH-type transcriptional activators and a PHA
361 synthesis repressor, suggests that extracellular mcl-PHA degradation activity of *B. vietnamiensis*
362 LMG 16232 may be integrated with other metabolic pathways. While we did not identify a specific
363 genetic element directly responsible for the uptake of mcl-PHA degradation products, we propose
364 passive diffusion. This hypothesis is based on the structural similarity between mcl-PHA
365 monomers and fatty acids, which both contain a hydrophobic alkyl chain (43). Medium-chain fatty
366 acids (C_7-C_{11}) can enter bacteria through simple diffusion without the involvement of active
367 transport systems or an unknown mechanism (44, 45) (**Fig. 9**).

368 Although our Tn-seq experiment was expected to saturate the whole genome, we cannot
369 rule out the possibility that the lipase production cluster (**Fig. 2**) may constitute a cold spot for
370 transposon insertions. Thus, this could decrease the probability of obtaining clones with insertions

371 in *lip2* having insertions with a halo of degradation. Furthermore, since *lip2* and *lipO* probably
372 form an operon, an insertion in *lip2* may not be informative about its function due to the potential
373 polar effect on *lipO*. Therefore, we took an *in silico* approach to analyze and compare the predicted
374 structures of Lip1 and Lip2. Our structural analysis of Lip1 and Lip2, based on AlphaFold
375 predictions, highlights a conserved core architecture and variable N- and C-terminal regions,
376 suggesting potential regulatory or accessory roles. The Predicted Aligned Error (PAE) matrices
377 confirm a stable domain architecture with flexible inter-domain regions, while high pLDDT values
378 reinforce confidence in the structural models. Superposition with 4LIP demonstrated overall
379 structural similarity but also revealed an obstructive alpha-helix in Lip1 and Lip2, which is absent
380 in 4LIP, which may influence enzyme activity. Further studies are needed to determine its
381 functional relevance. Both proteins maintain a conserved catalytic triad, consistent with lipase
382 activity. Docking experiments showed strong and specific binding for Lip1. In contrast, Lip2
383 exhibited multiple binding modes, indicating a more flexible binding pocket. A difference in the
384 amino acid at position 73: Lip1 contains glutamine (GLN), while Lip2 has tyrosine (TYR), which
385 may suggest reduced catalytic activity. Based on our experimental and docking results, Lip1
386 appears to function as an active lipase, while Lip2 may have altered activity due to structural
387 differences. Additional biochemical and structural studies are needed to validate these conclusions.

388 Overall this study provided new insight onto the degradation of extracellular mcl-PHA by
389 the genus *Burkholderia* thanks to a combination of activity screening, Tn-seq, and further
390 validation with RhaCAST.

391 **Material and methods**

392 *Strains, Selective Antibiotics, and Growth Conditions*

393 Strains and plasmids are shown in **Table 3**. Primers used in this study are listed in **Table**
394 **4**. All strains were grown in LB-Lennox medium (Difco). Strains of *Burkholderia* and the strains
395 of *E. coli* were initially grown at 37 °C, except for *E. coli* Stbl2, which was grown at 30 °C. The
396 following selective antibiotics were used: chloramphenicol (Sigma; 20 µg/mL for *E. coli*),
397 trimethoprim (Sigma; 100 µg/mL for strains of *Burkholderia*, 50 µg/mL for *E. coli*), gentamicin
398 (Sigma; 50 µg/mL for *Burkholderia*).

399 *Genomic and plasmid extraction*

400 Genomic DNA of the *B. vietnamiensis* LMG 16232 mutants made with RhaCAST were
401 extracted using the PureLink microbiome DNA purification kit (Invitrogen). Genomic DNA of the
402 Tn-seq pools were extracted using standard isopropanol precipitation. Plasmid DNA was extracted
403 using the EZNA Plasmid DNA Mini Kit (Omega Bio-tek). Both genomic and plasmid DNA were
404 eluted or solubilized in Tris-HCl pH 8.5.

405 *Substrate and media preparation*

406 The Poly(3-hydroxyoctanoate) (PHO) colloidal suspension was created by dissolving 400
407 mg of PHO into 200 mL acetone (Polyferm Canada Inc., Canada). Once the PHO was dissolved,
408 40 mL of dH_2O was added. The acetone was evaporated off using a speed evaporator. The colloidal
409 suspension was stored at 4˚ C until needed.

410 The mcl-PHA containing medium consisted of an M9 minimal medium agar (BD Difco,
411 USA) with 2 mM phenylalanine, 2 mM $MgSO_4$, 10 mg/ mL of PHO and 0.3 µg/mL Nile red. PHO
412 was added to the medium by using a previously prepared colloidal suspension of PHO. The PHO,
413 Nile red, $MgSO_4$, and phenylalanine were added after autoclaving to the M9 agar whilst melted.

414 25 mL of medium was then poured into petri plates. After solidifying, the plates were stored at
415 4°C until needed.

416 Tributyrin medium was made using a minimal medium with 2 mM phenylalanine and 2
417 mM $MgSO_4$ with tributyrin added to a final concentration of 4% (v/v) to the medium according to
418 the Sigma-Aldrich instructions (Sigma, St. Louis, Missouri, USA). The tributyrin was added after
419 autoclaving whilst the agar medium was around 80°C. The medium with tributyrin was vigorously
420 mixed until ready to pour into petri plates. After solidifying, the plates were stored at 4°C until
421 needed.

422 *Screening for mcl-PHA and tributyrin degradation*

423 To determine the strain's ability to degrade mcl-PHA and tributyrin degradation. The
424 overnight cultures were grown at 30°C and washed twice with PBS. 20 μL of the culture was
425 inoculated after being adjusted to an OD_{600} of 1. For mcl-PHA degradation determination, the
426 plates were incubated for 7-20 days; For tributyrin degradation determination, the plates were
427 incubated for 3 days, both incubated at 30°C. The visualization of the halo degradation was
428 performed using AlphaImager EP (Cell Biosciences, Santa Clara, CA). For the mcl-PHA plates
429 containing Nile red, the image was taken under UV excitation. Colonies that appeared to have lost
430 the PHO degradation activity on the first round of screening were then subjected to a secondary
431 screening to rule out false positives. 66 and 18 transconjugants were isolated without or with weak
432 PHO degradation activity, respectively. *Transposon mutagenesis, Tn-seq library preparation and*
433 *genome mapping*

434 *B. vietnamiensis* LMG 16232 was subjected to transposon mutagenesis with
435 pRBrhaBoutgfp (46). A total of 50,000 single colonies were screened. This number is based on
436 the expected average transposon insertion density from the model, approximately eight transposon

437 insertions per gene. Assuming a genome with N = 6000 non-essential genes and a collection of N
438 = 50,000 transposon insertion mutants, the probability that a single gene will see no transposon
439 insertions is: P(0, k, N) = e^(-50,000/6,000) = 2.4×10^{-4}; the total number of genes that will see no
440 insertions is: N* e^(-k/N) = 6,000 x 2.4×10^{-4} = 1.4 genes; and the total number of genes will be
441 found with this transposon density is n(insertion) 6,000* (1-e ^(-50,000/ 6,000)) = 5,999 genes.

442 Tn-seq was chosen to identify the transposon insertion sites. To enrich transposon-genome
443 junctions and to determine the insertion site, an adapted Tn-seq method, Tn-seq circle, developed
444 by Gallagher et al. (47), was performed as previously described with some minor modifications
445 (47, 48). Briefly, cultures of individual mutants were grown individually to approximately OD_{600}
446 of 3 and were combined into two separate pools, based on without (Pool 1) or with weak (Pool 2)
447 PHO degradation activity. The cultures were harvested, followed by the genomic DNA extraction.
448 The DNA was sheared to an average size of 300 bp via ultrasonication with a Covaris M220 (duty
449 factor of 20%, a peak incident power of 50W, 200 cycles per burst, and a duration of 75s), followed
450 by end repair with the NEBNext End Repair Module (NEB) and A-tailing. Next, the products were
451 ligated with adaptors, consisting of annealing oligos 683 and 684 with the Quick Ligation Kit
452 (NEB) and digested with *PacI* (NEB). Probe 682 in the presence of Ampligase (Lucigen) was used
453 to circularize fragments containing the transposon sequence. The exonuclease treatment was
454 carried out with a mix of T7 gene 6 exonuclease (ThermoFisher), Lambda exonuclease (NEB),
455 and Exonuclease I (NEB) to digest the linear fragments. The enrichment of the transposon–genome
456 junctions was confirmed by comparing the amplification of the transconjugant's pools with wild-
457 type *B. vietnamiensis* LMG 16232 using qPCR with iTaq Universal SYBR Green Supermix (Bio-
458 Rad). The number of PCR cycles corresponding to ~50% saturation by qPCR was chosen to
459 amplify transposon-genome junctions with iTaq DNA polymerases (Bio-Rad) for Illumina

460 sequencing. PCR primers 681, 690, 718, and 719 contain the Nextera indices and were used in
461 appropriate pairs (**Table 4**). The indexed samples were then cleaned-up with the SeraMag beads
462 (Cytiva), analysed on a TapeStation4150 (Agilent Technologies) and sequenced with an Illumina
463 MiSeq 2500. Raw reads were deposited in the NCBI Sequence Read Archive (SRA) repository
464 and will be publicly available after publication under BioProject: PRJNA1082765, accession:
465 SRR28216496 (Pool 1), SRR28216495 (Pool 2).

466 The sequenced reads of these mutants were mapped to the *B. vietnamensis* LMG 16232
467 genome with the Galaxy bioinformatics platform (https://usegalaxy.org). Using Cutadapt
468 (Galaxy v2.9+galaxy0) (49), the transposon sequence

469 5'-NNNNAATCTAGACTAGTGCGGCCGCACTTGTGTATAAGAGTCA-3' was removed
470 from the FASTQ file. Next, using Burrows-Wheeler transform (BWA) (Galaxy v0.7.17.4) (50),
471 the reads were mapped to the close genome of *B. vietnamiensis* LMG 16232 (25). The BWA's
472 BAM output was then converted to SAM using BAM-to-SAM (Galaxy 2.0.2) (51). The output
473 was visualized using Geneious 8.1.9.

474 *Determination of the PHO content beneath inoculated culture*

475 The inoculated culture from the phenotypic assay was scraped off from the agar. An agar
476 disk beneath the inoculated culture was cut using the back of the P1000 pipette tip. For control, a
477 disk was cut where no cell was inoculated. The samples were dried at 60°C for 16 hours, and the
478 PHO was extracted in chloroform using the acid-catalyzed methanolysis procedure as previously
479 described (52, 53). The determination of PHO in the agar was performed using an Agilent 7890A
480 gas chromatograph equipped with a DB-23 capillary column (30 m × 250 µm × 0.25 µm) and a
481 flame ionization detector (Agilent Technologies, Santa Clara, CA). Method operating parameters
482 and peak quantification have been previously described (52, 54).

483 *In silico analysis*

484 The calculated molecular weight and theoretical isoelectric point (pI) of the putative
485 enzyme were computed with Expasy (28). The putative catalytic amino acid was predicted with
486 Phyre2 server (Protein Homology/analogY Recognition Engine V 2.0) (55). Signal peptides were
487 predicted for predicted PHA depolymerases using Signal P 5.0
488 (https://services.healthtech.dtu.dk/service.php?SignalP) with default settings using both Gram-
489 negative and Gram-positive predictions (56). The alignment of amino acid sequences was
490 performed using Clustal Omega (https://www.ebi.ac.uk/jdispatcher/msa) (57). Protein
491 conformation was predicted using ColabFold 2 (58). Molecular docking studies were conducted
492 using Autodock 4 (59) to investigate the interaction between the enzyme and its potential
493 substrates. The docking protocol was guided by the crystal structure of the reference protein (PDB
494 ID: 4LIP). Visual representations of the predicted protein structures and docking interactions were
495 generated using PyMOL version 3.0.3 (60).

496 *Construction of B. vietnamiensis LMG 16232 insertional mutants*

497 Genes were interrupted using the RhaCAST method reported previously (24). Briefly, 24
498 bp crRNAs were designed from the genes to be targeted, and the templates were ordered as single-
499 stranded oligos and PCR-amplified using PCR primers 3392 and 3421 to create double-stranded
500 DNA fragments. The PCR products were then introduced into pRhaCAST using Golden Gate
501 cloning with SapI (NEB). The newly constructed plasmids were then transformed into *E. coli*
502 Stbl2. pRhaCAST was then introduced to *B. vietnamiensis* LMG 16232 by tetra-parental mating
503 (24). *E. coli* MM290/pRK2013 helper strain, *E. coli* Stbl2/pRhaCAST with corresponding crRNA,
504 and *E. coli* PIR1/pDonorTp was conjugated into *B. vietnamiensis* LMG 16232 on LB agar plate
505 containing 0.05% rhamnose. The plate was incubated at 37°C for 24 hours. Successful

506 exconjugants were selected on LB plates containing trimethoprim and gentamycin to select against
507 the *E. coli*. Colonies that appeared within 48 h at 37°C were screened by colony PCR. All
508 insertional mutants constructed with RhaCAST were verified by whole genome sequencing using
509 Oxford Nanopore Technologies platforms with v14 library prep chemistry and R10.4.1 flow cells
510 by Plasmidsaurus (Oregon, USA). The genomic sequence of the insertional mutants is available
511 after under BioProject: PRJNA1205771.

512 **Author Contributions**

513 STC and ZLY formulated the ideas and design of the project; GGL performed docking
514 experiment; ZLY and MS designed and cloned the plasmids and mutants; ZLY, MS, RD, and WB
515 performed phenotypic assays; ZLY and AMH performed library prep for Tn-seq. ZLY and AM
516 processed and analyzed the Tn-seq data; ZLY wrote the manuscript and edited together with STC,
517 GGL, MS, RD, AMH, AM, WB, RS, DBL, and DFDP; STC, DFDP, DBL, RS, and WB provided
518 financial support and supervised the work.

519 **Acknowledgements and Funding Sources**

520 This work was supported by a Natural Sciences and Engineering Research Council
521 (NSERC) of Canada Discovery Grant to SC and a University of Manitoba Collaborative Research
522 Program (UCRP) grant to SC and DBL. ZLY was supported by a Research Manitoba and
523 University of Manitoba Graduate Fellowship (UMGF); MS was supported by NSERC
524 Undergraduate Student Research Awards (USRA); AMH was supported by a Cystic Fibrosis
525 Canada studentship and a Canadian Institutes of Health Research (CIHR) Vanier award.

526 **Conflict of Interest Statement**

527 The authors declare no competing financial interests.

528 **References**

529 1. Muneer F, Rasul I, Azeem F, Siddique MH, Zubair M, Nadeem H. 2020. Microbial
530 Polyhydroxyalkanoates (PHAs): Efficient Replacement of Synthetic Polymers. J Polym Environ
531 28:2301–2323.

532 2. Li Z, Yang J, Loh XJ. 2016. Polyhydroxyalkanoates: opening doors for a sustainable future. NPG
533 Asia Mater 8:e265–e265.

534 3. Jendrossek D, Handrick R. 2002. Microbial degradation of polyhydroxyalkanoates. Annu Rev
535 Microbiol 56:403–432.

536 4. Jendrossek D. 2009. Polyhydroxyalkanoate Granules Are Complex Subcellular Organelles
537 (Carbonosomes). J Bacteriol 191:3195–3202.

538 5. Knoll M, Hamm TM, Wagner F, Martinez V, Pleiss J. 2009. The PHA Depolymerase Engineering
539 Database: A systematic analysis tool for the diverse family of polyhydroxyalkanoate (PHA)
540 depolymerases. BMC Bioinformatics 10:89.

541 6. Viljakainen VR, Hug LA. 2021. The phylogenetic and global distribution of bacterial
542 polyhydroxyalkanoate bioplastic-degrading genes. Environ Microbiol 23:1717–1731.

543 7. Schirmer A, Jendrossek D. 1994. Molecular characterization of the extracellular poly(3-
544 hydroxyoctanoic acid) [P(3HO)] depolymerase gene of Pseudomonas fluorescens GK13 and of its
545 gene product. J Bacteriol 176:7065–7073.

546 8. Kim DY, Kim HC, Kim SY, Rhee YH. 2005. Molecular characterization of extracellular medium-
547 chain-length poly(3-hydroxyalkanoate) depolymerase genes from Pseudomonas alcaligenes strains.
548 J Microbiol Seoul Korea 43:285–294.

549 9. Rhee YH, Kim YH, Shin K-S. 2006. Characterization of an extracellular poly (3-hydroxyoctanoate)
550 depolymerase from the marine isolate, *Pseudomonas luteola* M13-4. Enzyme Microb Technol
551 38:529–535.

552 10. Martínez V, de la Peña F, García-Hidalgo J, de la Mata I, García JL, Prieto MA. 2012. Identification
553 and Biochemical Evidence of a Medium-Chain-Length Polyhydroxyalkanoate Depolymerase in the
554 Bdellovibrio bacteriovorus Predatory Hydrolytic Arsenal. Appl Environ Microbiol 78:6017–6026.

555 11. Papaneophytou CP, Velali EE, Pantazaki AA. 2011. Purification and characterization of an
556 extracellular medium-chain length polyhydroxyalkanoate depolymerase from *Thermus*
557 *thermophilus* HB8. Polym Degrad Stab 96:670–678.

558 12. Martínez V, de Santos PG, García-Hidalgo J, Hormigo D, Prieto MA, Arroyo M, de la Mata I. 2015.
559 Novel extracellular medium-chain-length polyhydroxyalkanoate depolymerase from Streptomyces
560 exfoliatus K10 DSMZ 41693: a promising biocatalyst for the efficient degradation of natural and
561 functionalized mcl-PHAs. Appl Microbiol Biotechnol 99:9605–9615.

562 13. Gangoiti J, Santos M, Prieto MA, de la Mata I, Serra JL, Llama MJ. 2012. Characterization of a
563 Novel Subgroup of Extracellular Medium-Chain-Length Polyhydroxyalkanoate Depolymerases
564 from Actinobacteria. Appl Environ Microbiol 78:7229–7237.

565 14. Santos M, Gangoiti J, Keul H, Möller M, Serra JL, Llama MJ. 2013. Polyester hydrolytic and
566 synthetic activity catalyzed by the medium-chain-length poly(3-hydroxyalkanoate) depolymerase
567 from *Streptomyces venezuelae* SO1. Appl Microbiol Biotechnol 97:211–222.

568 15. Gupta R, Gupta N, Rathi P. 2004. Bacterial lipases: an overview of production, purification and
569 biochemical properties. Appl Microbiol Biotechnol 64:763–781.

570 16. Jaeger KE, Steinbüchel A, Jendrossek D. 1995. Substrate specificities of bacterial
571 polyhydroxyalkanoate depolymerases and lipases: bacterial lipases hydrolyze poly(omega-
572 hydroxyalkanoates). Appl Environ Microbiol 61:3113–3118.

573 17. Sharma PK, Mohanan N, Sidhu R, Levin DB. 2019. Colonization and degradation of
574 polyhydroxyalkanoates by lipase-producing bacteria. Can J Microbiol 65:461–475.

575 18. Rathi P, Saxena RK, Gupta R. 2001. A novel alkaline lipase from *Burkholderia cepacia* for
576 detergent formulation. Process Biochem 37:187–192.

577 19. Oliveira BH, Santos RÉ, Loiola LEA, Nascimento VMG. 2015. Overproduction and properties of
578 lipase by a wild strain of Burkholderia lata LBBIO-BL02 using chicken fat. 2. Ann Microbiol
579 65:865–877.

580 20. Shu Z, Wu J, Chen D, Cheng L, Zheng Y, Chen J, Huang J. 2012. Optimization of Burkholderia sp.
581 ZYB002 lipase production for pitch control in thermomechanical pulping (TMP) processes.
582 Holzforschung 66:341–348.

583 21. Lo C-F, Yu C-Y, Kuan I-C, Lee S-L. 2012. Optimization of Lipase Production by Burkholderia sp.
584 Using Response Surface Methodology. Int J Mol Sci 13:14889.

585 22. Yudistira H, McClarty L, Bloodworth RA, Hammond SA, Butcher H, Mark BL, Cardona ST. 2011.
586 Phenylalanine induces *Burkholderia cenocepacia* phenylacetic acid catabolism through degradation
587 to phenylacetyl-CoA in synthetic cystic fibrosis sputum medium. Microb Pathog 51:183–196.

588 23. Tung TT, Quoc Thang N, Cao Huy N, Bao Phuong P, Ngoc Minh D, Hai Nam N, Nielsen J. 2024.
589 Identification of novel phenylalanine derivatives bearing a hydroxamic acid moiety as potent
590 quorum sensing inhibitors. RSC Med Chem 15:1320–1328.

591 24. Yap ZL, Rahman ASMZ, Hogan AM, Levin DB, Cardona ST. 2024. A CRISPR-Cas-associated
592 transposon system for genome editing in Burkholderia cepacia complex species. Appl Environ
593 Microbiol 90:e0069924.

594 25. Yap ZL, Motnenko A, Cardona S. 2023. Complete Genome Sequence of Burkholderia
595 vietnamiensis LMG16232. Microbiol Resour Announc 12:e0032823.

596 26. Baym M, Shaket L, Anzai IA, Adesina O, Barstow B. 2016. Rapid construction of a whole-genome
597 transposon insertion collection for *Shewanella oneidensis* by Knockout Sudoku. Nat Commun 7:1–
598 13.

599 27. Mohanan N, Montazer Z, Sharma PK, Levin DB. 2020. Microbial and Enzymatic Degradation of
600 Synthetic Plastics. Front Microbiol 11:580709.

601 28. Gasteiger E, Hoogland C, Gattiker A, Duvaud S, Wilkins MR, Appel RD, Bairoch A. 2005. Protein
602 Identification and Analysis Tools on the ExPASy Server, p. 571–607. *In* Walker, JM (ed.), The
603 Proteomics Protocols Handbook. Humana Press, Totowa, NJ.

604 29. Mohanan N, Wong CH, Budisa N, Levin DB. 2022. Characterization of Polymer Degrading
605 Lipases, LIP1 and LIP2 From Pseudomonas chlororaphis PA23. Front Bioeng Biotechnol
606 10:854298.

607 30. Nor Azura Azam et al. 2018. Enhanced degradation of polyhydroxyalkanoates (PHAs) by newly
608 isolated *Burkholderia cepacia* DP1 with high depolymerase activity. 27 Apri 2017 75:11.

609 31. Azura Azami N, Ira Aryani W, Aik-Hong T, Amirul AA. 2019. Purification and characterization of
610 new bio-plastic degrading enzyme from *Burkholderia cepacia* DP1. Protein Expr Purif 155:35–42.

611 32. Sánchez DA, Tonetto GM, Ferreira ML. 2018. Burkholderia cepacia lipase: A versatile catalyst in
612 synthesis reactions. Biotechnol Bioeng 115:6–24.

613 33. Liu C-H, Huang C-C, Wang Y-W, Chang J-S. 2012. Optimizing lipase production from isolated
614 *Burkholderia* sp. J Taiwan Inst Chem Eng 43:511–516.

615 34. Li J, Shen W, Fan G, Li X. 2018. Screening, purification and characterization of lipase from
616 Burkholderia pyrrocinia B1213. 3 Biotech 8:387.

617 35. Alnoch RC, Cardoso RLA, Guizelini D, Balsanelli E, Tadra-Sfeir MZ, de Oliveira Pedrosa F,
618 Sassaki GL, Cruz LM, Mitchell DA, de Souza EM, Krieger N, Muller-Santos M. 2019. Genome
619 sequencing of Burkholderia contaminans LTEB11 reveals a lipolytic arsenal of biotechnological
620 interest. Braz J Microbiol 50:619–624.

621 36. Park O-J, Lee S-H. 2005. Stereoselective lipases from *Burkholderia* sp., cloning and their
622 application to preparation of methyl (*R*)-*N*-(2,6-dimethylphenyl)alaninate, a key intermediate for
623 (*R*)-Metalaxyl. J Biotechnol 120:174–182.

624 37. Lee S-H, Kim M-N. 2010. Isolation of bacteria degrading poly(butylene succinate-*co*-butylene
625 adipate) and their *lip A* gene. Int Biodeterior Biodegrad 64:184–190.

626 38. Knapp A, Voget S, Gao R, Zaburannyi N, Krysciak D, Breuer M, Hauer B, Streit WR, Müller R,
627 Daniel R, Jaeger K-E. 2015. Mutations improving production and secretion of extracellular lipase
628 by Burkholderia glumae PG1. Appl Microbiol Biotechnol 100:1265.

629 39. Khattabi ME, Gelder PV, Bitter W, Tommassen J. 2000. Role of the Lipase-specific Foldase of
630 Burkholderia glumae as a Steric Chaperone. J Biol Chem 275:26885–26891.

631 40. Wang X, Yu X, Xu Y. 2009. Homologous expression, purification and characterization of a novel
632 high-alkaline and thermal stable lipase from *Burkholderia cepacia* ATCC 25416. Enzyme Microb
633 Technol 45:94–102.

634 41. Frenken LGJ, de Groot A, Tommassen J, Verrips CT. 1993. Role of the lipB gene product in the
635 folding of the secreted lipase of Pseudomonas glumae. Mol Microbiol 9:591–599.

636 42. Cuthbertson L, Nodwell JR. 2013. The TetR Family of Regulators. Microbiol Mol Biol Rev
637 77:440–475.

638 43. Kniewel R, Revelles Lopez O, Prieto MA. 2017. Biogenesis of Medium-Chain-Length
639 Polyhydroxyalkanoates, p. 1–25. *In* Geiger, O (ed.), Biogenesis of Fatty Acids, Lipids and
640 Membranes. Springer International Publishing, Cham.

641 44. Black PN, DiRusso CC. 1994. Molecular and biochemical analyses of fatty acid transport,
642 metabolism, and gene regulation in *Escherichia coli*. Biochim Biophys Acta 1210:123–145.

643 45. Jimenez-Diaz L, Caballero A, Segura A. 2017. Pathways for the Degradation of Fatty Acids in
644 Bacteria, p. 1–23. *In* Rojo, F (ed.), Aerobic Utilization of Hydrocarbons, Oils and Lipids. Springer
645 International Publishing, Cham.

646 46. Cardona ST, Mueller C, Valvano MA. 2006. Identification of essential operons in *Burkholderia*
647 *cenocepacia* with a rhamnose inducible promoter. Appl Environ Microbiol 72:2547–2555.

648 47. Gallagher LA, Shendure J, Manoil C. 2011. Genome-scale identification of resistance functions in
649 *Pseudomonas aeruginosa* using Tn-seq. mBio 2:e00315-10.

650 48. Gislason AS, Turner K, Domaratzki M, Cardona ST. 2017. Comparative analysis of the
651 *Burkholderia cenocepacia* K56-2 essential genome reveals cell envelope functions that are uniquely
652 required for survival in species of the genus *Burkholderia*. Microb Genomics 3:e000140.

653 49. Martin M. 2011. Cutadapt removes adapter sequences from high-throughput sequencing reads. 1.
654 EMBnet.journal 17:10–12.

655 50. Li H, Durbin R. 2010. Fast and accurate long-read alignment with Burrows–Wheeler transform.
656 Bioinformatics 26:589–595.

657 51. Li H, Handsaker B, Wysoker A, Fennell T, Ruan J, Homer N, Marth G, Abecasis G, Durbin R,
658 Subgroup 1000 Genome Project Data Processing. 2009. The Sequence Alignment/Map format and
659 SAMtools. Bioinformatics 25:2078–2079.

660 52. Fu J, Sharma U, Sparling R, Cicek N, Levin DB. 2014. Evaluation of medium-chain-length
661 polyhydroxyalkanoate production by Pseudomonas putida LS46 using biodiesel by-product streams.
662 Can J Microbiol 60:461–468.

663 53. Braunegg G, Sonnleitner B, Lafferty RM. 1978. A rapid gas chromatographic method for the
664 determination of polyhydroxybutyric acid in microbial biomass. Eur J Appl Microbiol Biotechnol
665 6:29–37.

666 54. Blunt W, Lagassé A, Harvey J, Sparling R, Gapes D, Levin D, Cicek N. 2024. Semi-continuous
667 non-sterile production of medium chain-length polyhydroxyalkanoates from fatty acids. Can J
668 Chem Eng 102:3896–3908.

669 55. Kelley LA, Mezulis S, Yates CM, Wass MN, Sternberg MJE. 2015. The Phyre2 web portal for
670 protein modeling, prediction and analysis. Nat Protoc 10:845–858.

671 56. Almagro Armenteros JJ, Tsirigos KD, Sønderby CK, Petersen TN, Winther O, Brunak S, von
672 Heijne G, Nielsen H. 2019. SignalP 5.0 improves signal peptide predictions using deep neural
673 networks. Nat Biotechnol 37:420–423.

674 57. Madeira F, Madhusoodanan N, Lee J, Eusebi A, Niewielska A, Tivey ARN, Lopez R, Butcher S.
675 2024. The EMBL-EBI Job Dispatcher sequence analysis tools framework in 2024. Nucleic Acids
676 Res 52:W521–W525.

677 58. Kim G, Lee S, Levy Karin E, Kim H, Moriwaki Y, Ovchinnikov S, Steinegger M, Mirdita M. 2025.
678 Easy and accurate protein structure prediction using ColabFold. Nat Protoc 20:620–642.

679 59. Morris GM, Huey R, Lindstrom W, Sanner MF, Belew RK, Goodsell DS, Olson AJ. 2009.
680 AutoDock4 and AutoDockTools4: Automated docking with selective receptor flexibility. J Comput
681 Chem 30:2785–2791.

682 60. DeLano WL. 2002. Pymol: An open-source molecular graphics tool. CCP4 Newsl Protein
683 Crystallogr.

684 61. Darling P, Chan M, Cox AD, Sokol PA. 1998. Siderophore production by cystic fibrosis isolates of
685 *Burkholderia cepacia*. Infect Immun 66:874–877.

686 62. Bloodworth RA, Gislason AS, Cardona ST. 2013. *Burkholderia cenocepacia* conditional growth
687 mutant library created by random promoter replacement of essential genes. MicrobiologyOpen
688 2:243–258.

689 63. Figurski DH, Helinski DR. 1979. Replication of an origin-containing derivative of plasmid RK2
690 dependent on a plasmid function provided in trans. Proc Natl Acad Sci U S A 76:1648–1652.

691

692 **Figures and Legends**

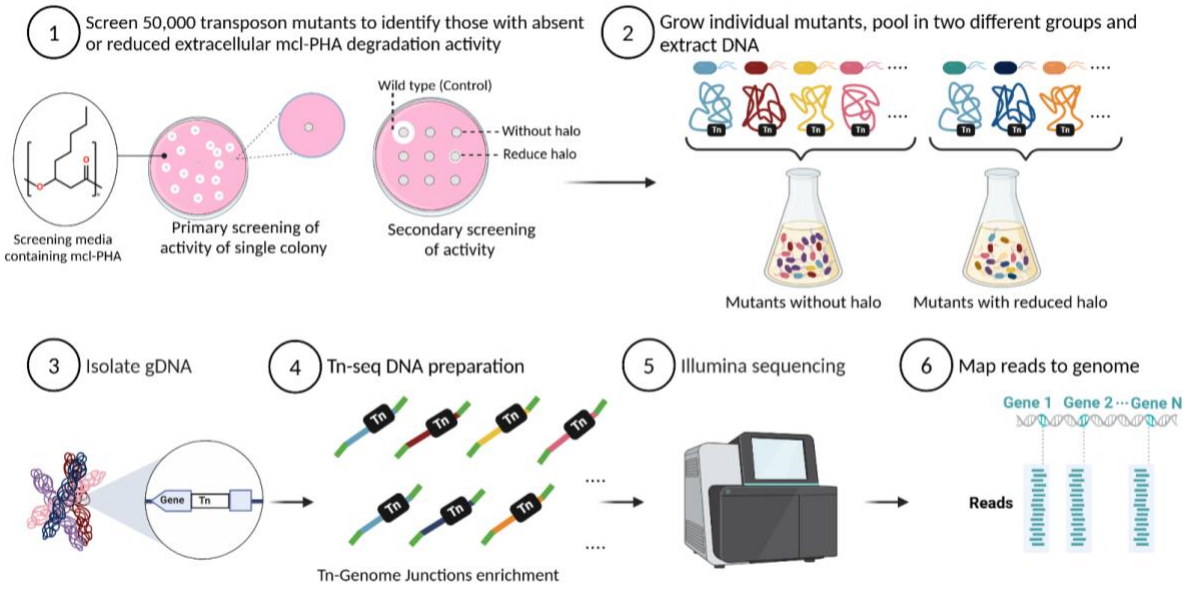

693

694 **Fig 1.** Overview of transposon mutagenesis and Tn-seq workflow to identify genetic elements
695 involved in the extracellular mcl-PHA degradation activity in *B. vietnamiensis* LMG 16232. *B.*
696 *vietnamiensis* LMG 16232 was subjected to transposon mutagenesis, and 50,000 colonies were
697 screened for those with absent or reduced extracellular mcl-PHA degradation activity. Colonies
698 showing reduced or no degradation activity were selected for further analysis. Selected mutants
699 were grown individually and then grouped into two pools based on their mcl-PHA degradation
700 activity (Pool 1 for no activity, Pool 2 for weak activity). Genomic DNA (gDNA) was extracted
701 from each pool. The gDNA was prepared for Tn-Genome junction enrichment. The enriched DNA
702 fragments were sequenced using Illumina MiSeq. The sequencing data were analyzed by mapping
703 the reads to the *B. vietnamiensis* LMG 16232 genome.

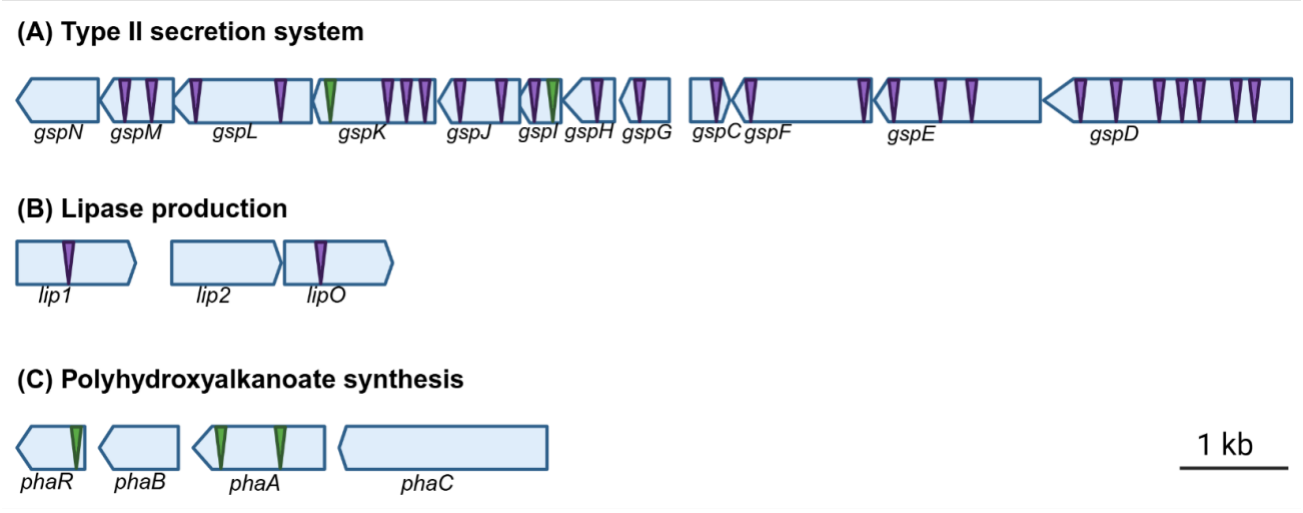

Fig 2. Genetic Organization of the *B. vietnamiensis* LMG 16232 gene clusters that affect the extracellular mcl-PHA degradation upon interruption by transposon insertion. The triangles indicate transposon insertions that resulted in the complete loss (Pool 1, purple) or severe reduction (Pool 2, green) of extracellular mcl-PHA degradation activity in *B. vietnamiensis* LMG 16232. (A) The type II secretion system of *B. vietnamiensis* LMG 16232 arranges in a gene cluster containing 12 genes (P4G95_05480, P4G95_05485, P4G95_05490, P4G95_05495, P4G95_05500, P4G95_05505, P4G95_05510, P4G95_05515, P4G95_05520, P4G95_05525, P4G95_05530, P4G95_05535). All genes of the gene cluster are interrupted except for *gspN*. (B) lipase gene cluster consists of three genes, *lip1, lip2* and *lipO* (P4G95_16805, P4G95_16810, and P4G95_16815). Interruption of *lip1* and *lipO* by transposon abolishes *B. vietnamiensis* LMG 16232 ability to degrade extracellular mcl-PHA. (C) The polyhydroxyalkanoate synthesis gene cluster of *B. vietnamiensis* LMG 16232 consists of four genes, *phaR, phaB, phaA, and phbC* (P4G95_13560, P4G95_13565, P4G95_13570, and P4G95_13575). Transposon interruption on *phaR* and *phaA* severely reduces *B. vietnamiensis* LMG 16232 to degrade extracellular mcl-PHA. The genes are depicted to scale, as indicated by the bars on the right side of the panels. The putative function of genes interrupted by transposon is provided in Table 2.

```
WHU94860.1     MVRSMRSRV-----------------------------VAAAVACAMSGAQFAGTTAVM   30
AFQ93688.1     ------------------------------------------------------------   0
AFQ93689.1     ------------------------------------------------------------   0
CAE81078.1     ----MKKLLAGVFGVVAMSLSAQAAKKASNCEVT----GLVDRMTCPYLEKL-VSGP-HL   50
AAA64538.1     --MPLRTLLCGLLLAVCLGQHALA---ASRCSERPRTLLRPAEVSCSYQSTWLDSGL-VG   54

WHU94860.1     TLATTHAATAATAATDDYAATRYPVILVH-GL-TGTDKYA---GVL-EYW--YGIQEDLQ   82
AFQ93688.1     ----VHTF-YH-PRAMGASGERHPVVIW-----------GNGTGAVPGIY--SSLLRHWA   41
AFQ93689.1     ----VHTF-YH-PRSMGASGERHPVVIW-----------GNGTGAVPGIY--SSLLRHWA   41
CAE81078.1     ---TRHVK-YSLPKGKTPKA-GWPTVILYQGSLFPVE-FSRSSLMIAGGYNEIRLIQTLL   104
AAA64538.1     ---QRKII-YQTPLGTPPAG-GWPVVLIYQGSFFPLNDFSYHSNLPFGGYYEGKLVQNLL   109
                    :             .   *.::            .         :    : .

WHU94860.1     RHGATVY----------VANLSGFQSD----DGPNGRGEQLLAYVKTVLAATGATKVNLI   128
AFQ93688.1     SHGFIVAAANTPTSNFALS----------MRAGIDVLERRNADPGSEYFGRVDLARIGSA   91
AFQ93689.1     SHGIIVAAANTPTSNFAIS----------MRAGIDVLERRNADPGSEYFGRVDLEHIGSA   91
CAE81078.1     DSGFAVIAPPAIEGVAWMTNIVGI--DYDTSEDFYFVEELLVAMGNGEFGKLNMDRLYAT   162
AAA64538.1     DHGYAVIAPSAPADLFWQTNIPGLAQAYELSTDYDFLGNVLAAIASGHFGPLNAQRQYAT   169
                 *  *           :             .     .      .  :.  .  :

WHU94860.1     GHSQGGLTSRYVAAVAPDLVASVTTIGTPHRGSEFADFVQSVLAYDPTGLSSSVIATFFN   188
AFQ93688.1     GHSQGGAAAVNAAVDAR-VDTAVPIQ-----PG--------PL-----TDP---------   123
AFQ93689.1     GHSQGGAAAVNAAIDAR-VDTAVPIQ-----PG--------PL-----TDP---------   123
CAE81078.1     GISSGGYHSSRMAVAFPGVFKALAVH-----SASYADCGG-PMCFVPAQVP---------   207
AAA64538.1     GISSGGYNTSRMAVSFPGKFRALAVQ-----SGSYATCSG-PLCVVPDQLP---------   214
               * *.**  :   *        ::         .         :

WHU94860.1     VFGILTSSSNNTNQDALAALKTLTTSQAAAYNQNYPSAGLGAPGSCQTGAPTETVGGNTH   248
AFQ93688.1     ---------------------------------------------DLTGVPVFY------   132
AFQ93689.1     ---------------------------------------------DLTDVPMFY------   132
CAE81078.1     ---------------------------------------------ENHPPTIF------   215
AAA64538.1     ---------------------------------------------ADHPPTLF------   222
                                                                  *

WHU94860.1     LLYSWAGTAIQPTVSMFGVTGAKDVSTIPVIDPANALDLSTLALLGTGTVMINRGAGQND   308
AFQ93688.1     ------------------LAGERDLTVWPAL----VKALYRDSD----------------   154
AFQ93689.1     ------------------LAGQRDLTVWPAL----VKALYRDSS----------------   154
CAE81078.1     ------------------LHGRLDPVV-PVR----TMYPYHETL----------------   236
AAA64538.1     ------------------LHGFVDAVV-PWW----SMDLYYDRL----------------   243
                                 : *  *  . *

WHU94860.1     GLVSKCSALYGQVLGTRYKWNHLDEINQLLGVRGAYAEDPVAVIRTHANRLKLAGV       364
AFQ93688.1     ----HLPAVYGEVRGAGHLS--------SIGDGGDFRAPT-TA-------------       184
AFQ93689.1     ----HLPAVYGEVRGAGHLS--------SIGDGGDFRAPT-T--------------       183
CAE81078.1     ----KNQG----VETEMFVS--------PWARHEWLEEAPELITNWFINHK-----       271
AAA64538.1     ----LHQG----IETARYTE--------PLGGHEWFAASPGKVLAWFNAHP-----       278
                     .    :    .            .
```

721

722 **Fig 3.** Amino acid sequence alignment of the putative lipase that is able to degrade extracellular
723 mcl-PHA depolymerase of *B. vietnamiensis* LMG 16232 (protein ID: WHU94860.1) with other
724 mcl-PHA depolymerase sequences. The sequences analyzed include those from *Streptomyces*
725 *roseolus* (GenBank: AFQ93688.1), *Streptomyces venezuelae* (GenBank: AFQ93689.1),
726 *Bdellovibrio bacteriovorus* HD100 (GenBank: CAE81078.1), *Pseudomonas fluorescens*
727 (GenBank: AAA64538.1). The lipase box consists of the pentapeptide sequence (G-X1-S-X2-G),
728 which is indicated in the red box. The signal peptide of *B. vietnamiensis* LMG 16232 was predicted
729 by the SignalP (version 5.0) program (purple box). The main putative catalytic amino acids
730 Ser131-Asp308-His330 of *B. vietnamiensis* LMG 16232, predicted with Phyre 2, are marked with
731 a dark blue box.

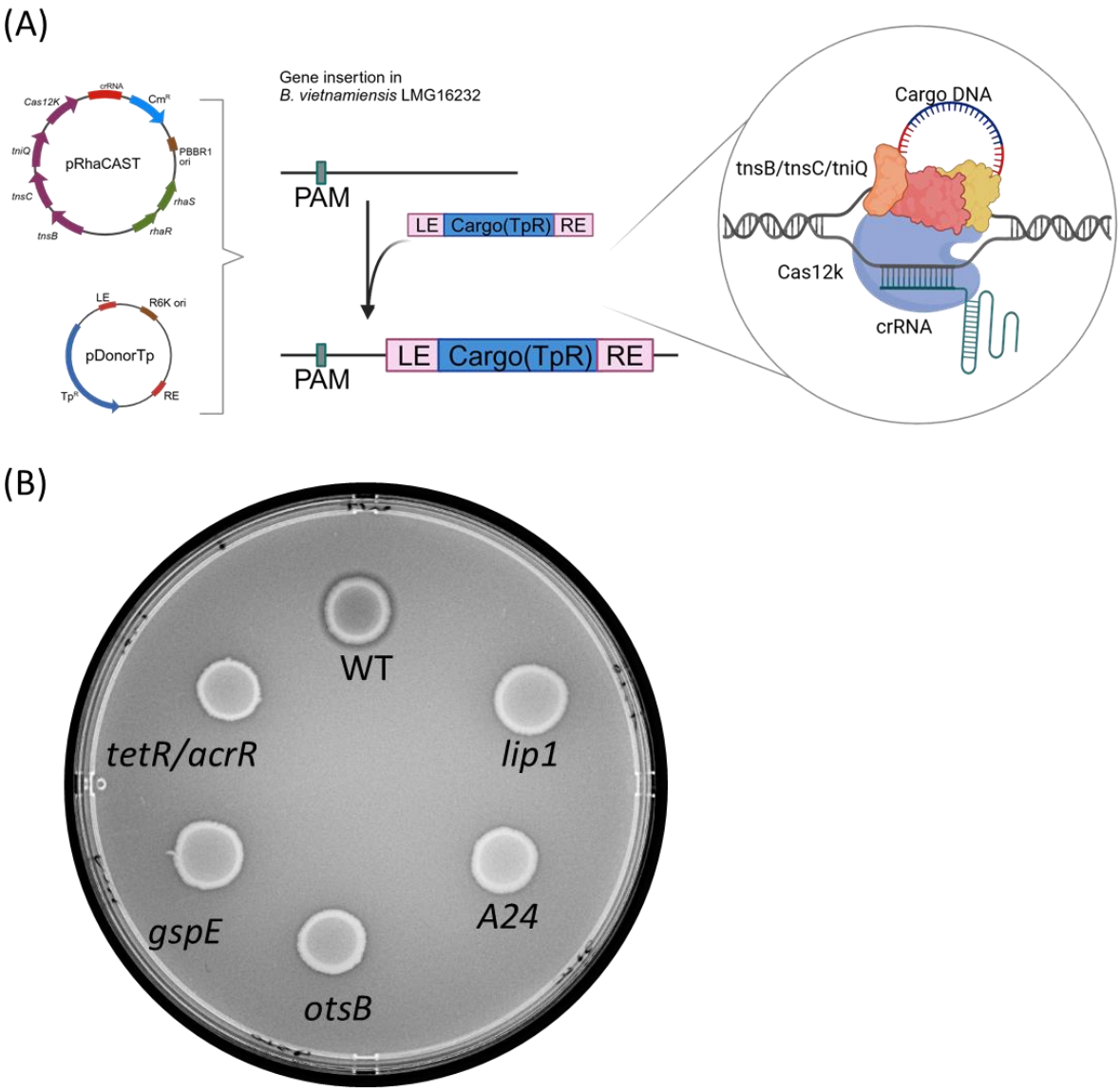

Fig 4. Targeting genes involved in mcl-PHA degradation in *B. vietnamiensis* LMG 16232 abolish the strain's ability to degrade mcl-PHA. (A) Schematic model of RNA-guided DNA transposition by RhaCAST applied to *B. vietnamiensis* LMG 16232. The two plasmids of the RhaCAST system, pRhaCAST and pDonorTp, encode all the necessary components, tnsB, tnsC, tniQ, Cas12k, crRNA scaffold, and the cargo gene (TpR) that is flanked by the transposon left end (LE) and right end (RE). (B) The ability to degrade mcl-PHA was ablated by CAST targeting triacylglycerol lipase CDS (*lip1*), A24 family peptidase CDS (*A24*), *otsB, gspE,* TetR/AcrR family transcriptional

740 regulator CDS (*tetR/acrR*) in LMG 16232 Wild-type (WT). This figure shows a representative

741 plate of the mcl-PHA degradation assay of three biological replicates in duplicates.

742

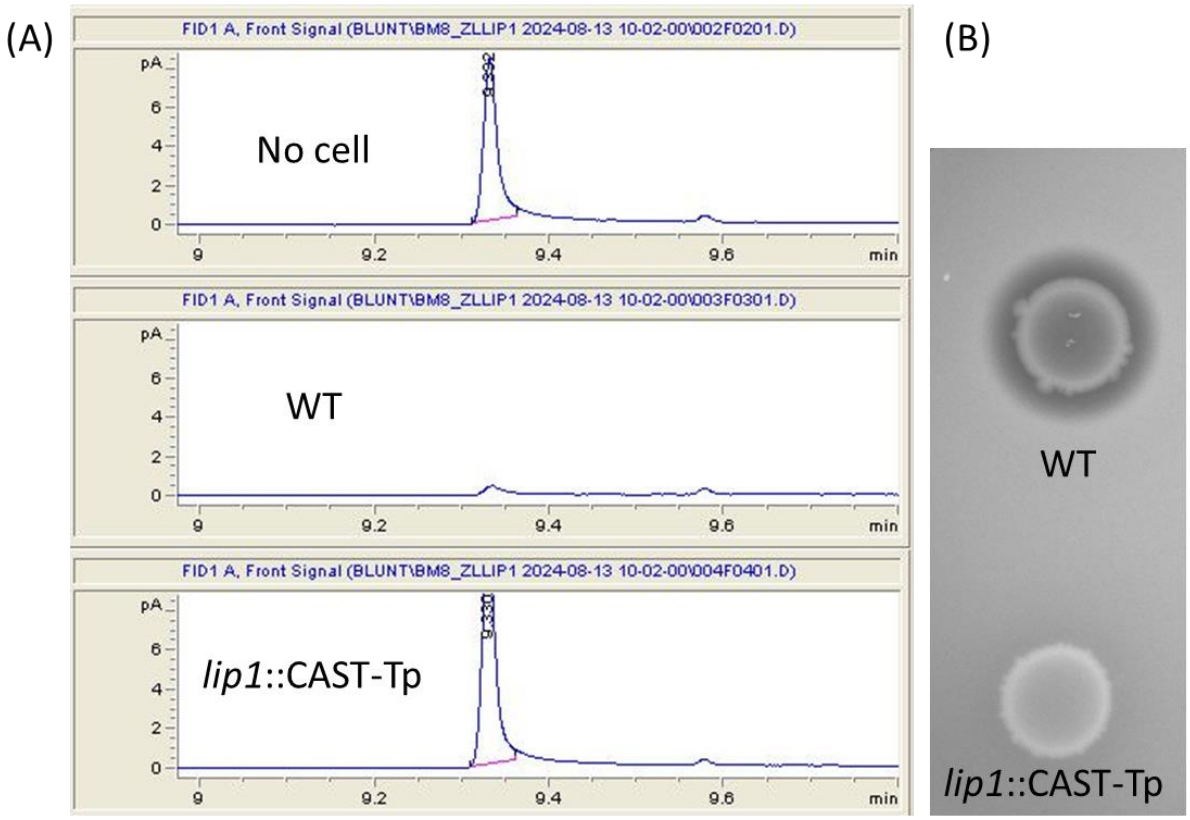

Fig 5. Targeting the putative *lipase* gene (locus tag: P4G95_16805) in *B. vietnamiensis* LMG 16232 abolishes the ability to degrade mcl-PHA. (A) Strains were grown on an agar plate containing Nile red and PHO and visualized under UV irradiation. Inoculation of wild type (WT) results in a clear halo around the strain, whereas the inoculation of the mutant *lip1::CAST-Tp* does not have a halo around the strain. (B) The absence or presence of PHO in the agar after strain inoculation was determined with gas chromatography with flame ionization detection (GC-FID). Samples were obtained by cutting an agar disk under the strain. For control, a disk was cut at an area of the agar where no cell was inoculated. The peak at ~9.3 minutes retention time corresponds to PHO, which can be observed at the no cell control (Top). The absence of a peak corresponds to PHO in WT, and the presence of PHO in *lip1::CAST-Tp* supports the phenotypic test.

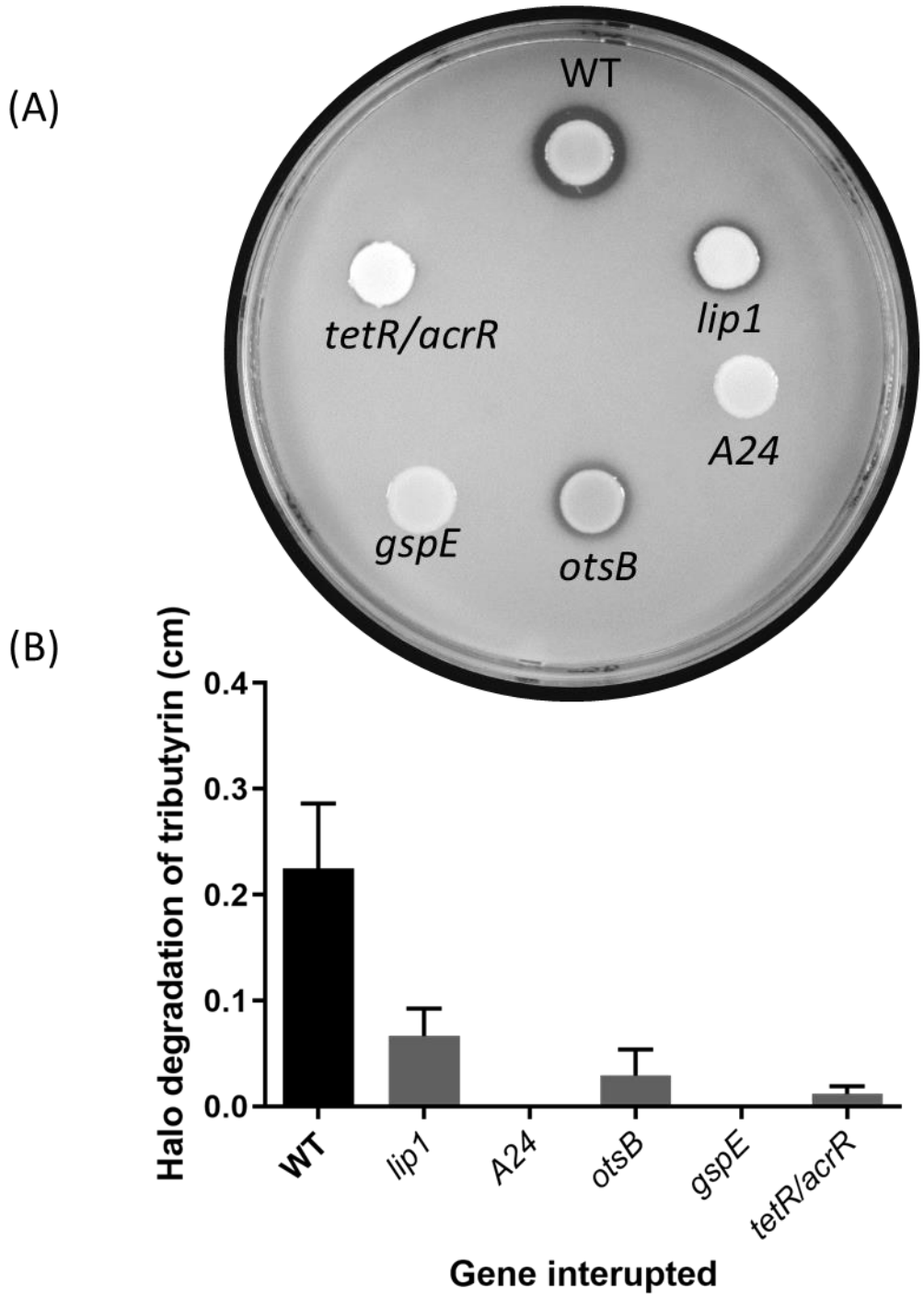

754

755 **Fig 6.** Targeting genes involved in mcl-PHA degradation in *B. vietnamiensis* LMG 16232 affects
756 the ability to degrade tributyrin. A) Representative plate of tributyrin degradation assay; B)
757 Diameter of the halos degradation in (A). The ability to degrade tributyrin was ablated by CAST
758 targeting triacylglycerol lipase CDS (*lip1*), A24 family peptidase CDS (*A24*), *otsB, gspE,*

759 TetR/AcrR family transcriptional regulator CDS (*tetR/acrR*) in LMG 16232 wild-type (WT). Data

760 is representative of two biological replicates repeated in technical triplicate.

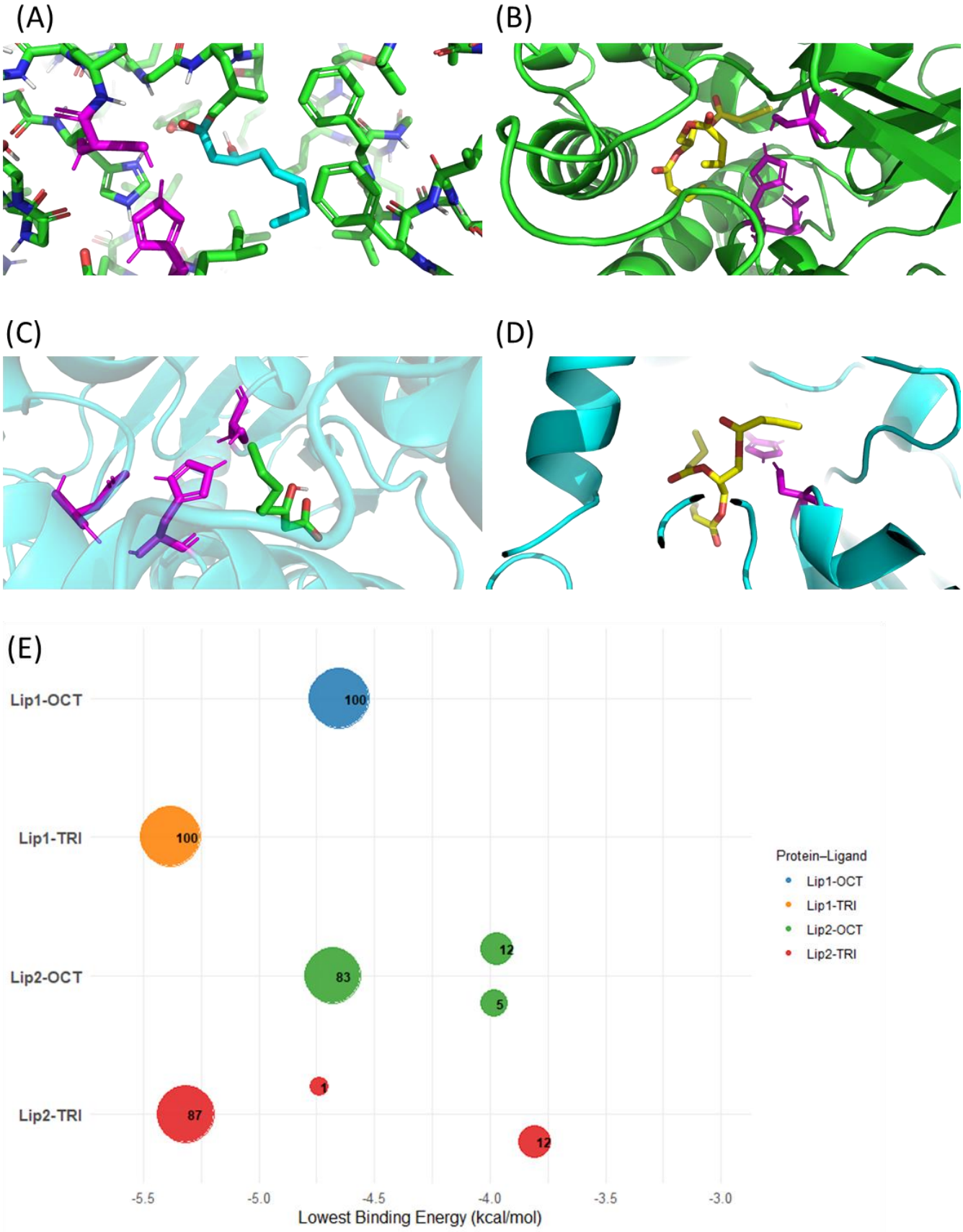
(A)
(B)
(C)
(D)
(E)
Lip1-OCT
Lip1-TRI
Lip2-OCT
Lip2-TRI
100
100
83
12
5
1
87
12
-5.5
-5.0
-4.5
-4.0
-3.5
-3.0
Lowest Binding Energy (kcal/mol)
Protein–Ligand
Lip1-OCT
Lip1-TRI
Lip2-OCT
Lip2-TRI

761

762 **Fig. 7** Docking analysis of Lip1 and Lip2-substrate complexes. A) Docking poses of Lip1 with 3-
763 Hydroxyoctanoate (OCT). B) Docking poses of Lip1 with Tributyrin (TRI). C) Docking poses of
764 Lip2 with 3-Hydroxyoctanoate (OCT). D) Docking poses of Lip2 with Tributyrin (TRI). The
765 images illustrate the single predominant low-energy binding cluster obtained for both substrates,
766 highlighting the catalytic triad in violet. (E) Binding energy and cluster distribution for protein-
767 ligand complexes. The plot shows the lowest binding energy for Lip1 and Lip2 docking with 3-
768 Hydroxyoctanoate (OCT) and Tributyrin (TRI). The size of the circle represents the cluster size
769 (number of poses), while colours differentiate protein-ligand pairs: Lip1-OCT (blue), Lip1-TRI
770 (orange), Lip2-OCT (green), and Lip2-TRI (red). Lip1 exhibits a higher affinity for both ligands,
771 characterized by a single predominant low-energy cluster, whereas Lip2 displays multiple binding
772 modes for both substrates.

773

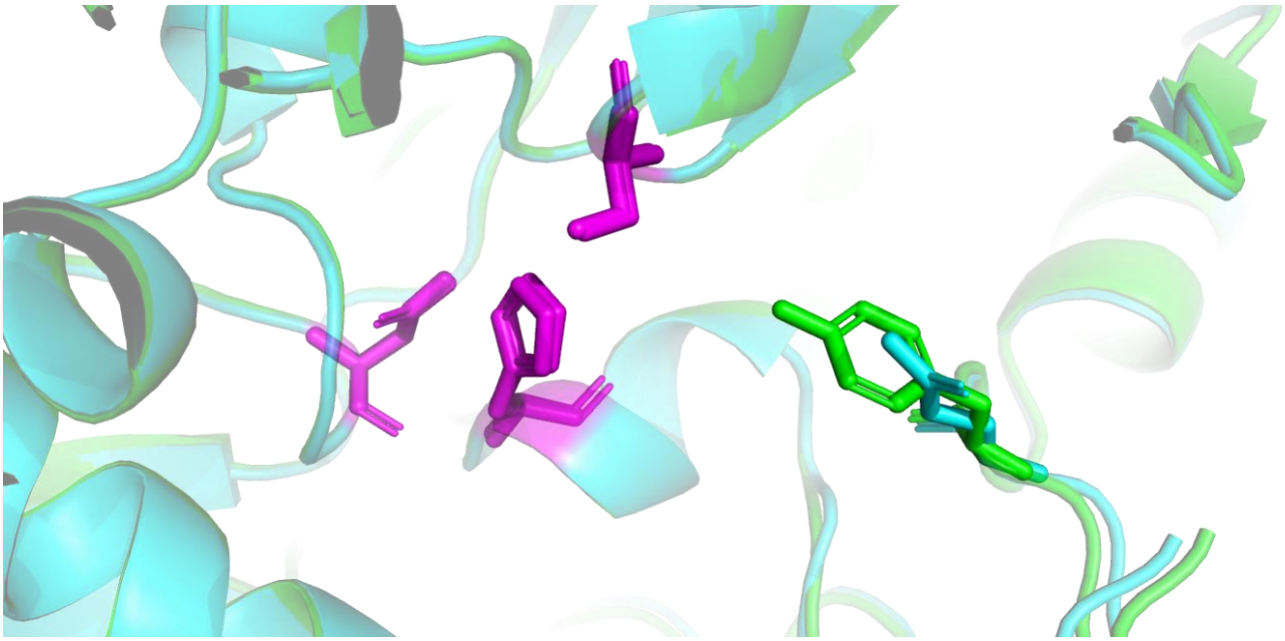

Fig 8. Structural superposition of Lip1 and Lip2 at amino acid at position 73. Superposition of Lip1 (green) and Lip2 (blue), highlighting the catalytic triad (violet) and the difference in amino acid in position 73: Lip1 (TYR) and Lip2 (GLN), illustrating its potential impact on enzyme structure and function.

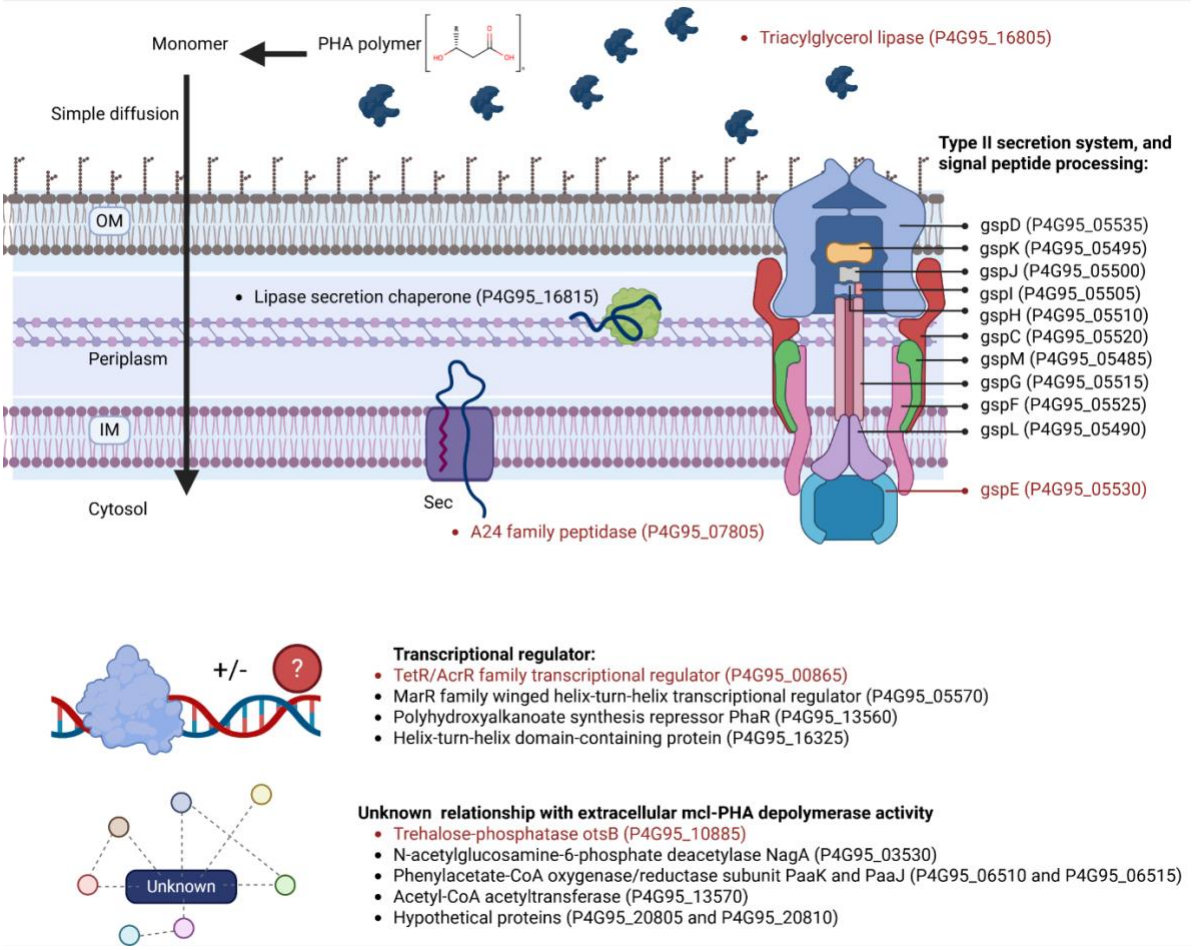
Monomer
PHA polymer
Triacylglycerol lipase (P4G95_16805)
Simple diffusion
Type II secretion system, and signal peptide processing:
OM
gspD (P4G95_05535)
gspK (P4G95_05495)
gspJ (P4G95_05500)
gspI (P4G95_05505)
gspH (P4G95_05510)
gspC (P4G95_05520)
gspM (P4G95_05485)
gspG (P4G95_05515)
gspF (P4G95_05525)
gspL (P4G95_05490)
Lipase secretion chaperone (P4G95_16815)
Periplasm
IM
Cytosol
Sec
A24 family peptidase (P4G95_07805)
gspE (P4G95_05530)
+/-
?
Transcriptional regulator:
TetR/AcrR family transcriptional regulator (P4G95_00865)
MarR family winged helix-turn-helix transcriptional regulator (P4G95_05570)
Polyhydroxyalkanoate synthesis repressor PhaR (P4G95_13560)
Helix-turn-helix domain-containing protein (P4G95_16325)
Unknown
Unknown relationship with extracellular mcl-PHA depolymerase activity
Trehalose-phosphatase otsB (P4G95_10885)
N-acetylglucosamine-6-phosphate deacetylase NagA (P4G95_03530)
Phenylacetate-CoA oxygenase/reductase subunit PaaK and PaaJ (P4G95_06510 and P4G95_06515)
Acetyl-CoA acetyltransferase (P4G95_13570)
Hypothetical proteins (P4G95_20805 and P4G95_20810)

779

780

781 **Fig 9.** Proposed model of components involved in *B. vietnamiensis* LMG 16232 extracellular mcl-
782 PHA degradation activity. The elements in this model were deduced from the transconjugants that
783 either lost or showed severely reduced extracellular mcl-PHA depolymerase activity due to
784 transposon insertion. The components where the text is in red have been verified via the creation
785 of insertional mutagenesis using RhaCAST. The regulatory elements influencing this activity are
786 TetR/AcrR family transcriptional regulator (P4G95_00865), Polyhydroxyalkanoate synthesis
787 repressor (P4G95_13560) and HTH-type regulators (P4G95_05570 and P4G95_16325). The Sec
788 system is responsible for transporting the unfolded protein into the periplasmic, as the protein is
789 predicted to contain a sec tag. The putative lipase chaperone (P4G95_16815) is responsible for
790 folding the putative lipase into a mature protein and excreted to the outside of the cell via the type
791 II secretion system. *B. vietnamiensis* LMG 16232 extracellular mcl-PHA degradation activity is
792 also affected by the transposon interruption in genetic elements related to polyhydroxyalkanoate
793 production and several genes involved in metabolism.

Table 1. *Burkholderia* isolates that exhibit extracellular mcl-PHO degradation activity

Species	Strain	Ability to degrade PHO after 20 days	
		30 ˚C	37 ˚C
Burkholderia cenocepacia	K56-2	-	-
	F9141525	-	-
	F3071909	-	-
	G1181568-1	-	-
	F4200989-3	-	-
	VC14488	-	-
	VC14543	-	-
	VC10414	-	-
	VC14761	-	-
	130723	-	-
	125007	-	-
Burkholderia contaminans	21NG595759	-	-
	21NG609698	-	-
Burkholderia dolosa	AU6940	-	-
	AU2167	-	-
	LM018941	-	-
	AU0645	-	-
Burkholderia gladioli	VC19233	+	+
	VC14812	-	-
	132208	+	-
	113611	-	-
Burkholderia multivorans	21NH942533	+	+
	21NJ503211	+	-
	V1120157	-	-
	LM013010	-	-
	F9091687	+	-
	VC19694	-	-
	VC15555	-	-
	VC9825	+	+
	131077	-	-
Burkholderia stagnalis	MSMB618	++	++
	MSMB642	++	++
Burkholderia vietnamiensis	LMG 22486	-	-
	LMG 10929	-	-
	LMG 16232	++	++
	VC11431	-	-
	VC18984	-	-

794 mcl-PHA degradation was ranked based on (–) no clearing, (+) weak clearing, (++) moderate
795 clearing. Fig. S1 is the source of the data interpretation.

Table 2. Transposon mutant of *B. vietnamiensis* LMG 16232 with abolished (Pool 1) or reduced (Pool 2) extracellular mcl-PHA activity

Chromosome location	Locus tag	Gene name	Putative function
Pool 1			
1	P4G95_00865	TetR/AcrR family transcriptional regulator CDS	TetR/AcrR family transcriptional regulator
1	P4G95_05485	gspM	type II secretion system protein M
1	P4G95_05490	gspL	type II secretion system protein GspL
1	P4G95_05495	gspK	type II secretion system minor pseudopilin GspK
1	P4G95_05500	gspJ/prepilin-type N-terminal cleavage/methylation domain-containing protein CDS	prepilin-type N-terminal cleavage/methylation domain-containing protein
1	P4G95_05505	gspI	type II secretion system minor pseudopilin GspI
1	P4G95_05510	GspH/FimT family pseudopilin CDS	GspH/FimT family pseudopilin
1	P4G95_05515	gspG	type II secretion system major pseudopilin GspG
1	P4G95_05520	general secretion pathway protein GspC CDS	general secretion pathway protein GspC CDS
1	P4G95_05525	gspF	type II secretion system inner membrane protein GspF
1	P4G95_05530	gspE	type II secretion system ATPase GspE
1	P4G95_05535	gspD	type II secretion system secretin GspD
1	P4G95_07805	A24 family peptidase CDS	A24 family peptidase
1	P4G95_10885	otsB CDS	trehalose-phosphatase
2	P4G95_16805	lip1/triacylglycerol lipase CDS	triacylglycerol lipase
2	P4G95_16815	lipO/lipase secretion chaperone CDS	lipase secretion chaperone
2	P4G95_20805	hypothetical protein CDS	hypothetical protein
3	P4G95_28980	gspD CDS	type II secretion system secretion GspD
Pool 2			
1	P4G95_03530	nagA	N-acetylglucosamine-6-phosphate deacetylase
1	P4G95_05495	gspK	type II secretion system minor pseudopilin GspK
1	P4G95_05505	gspI	type II secretion system minor pseudopilin GspI

1	Between P4G95_05555 and P4G95_05560	Between mnmC and cation:proton antiporter CDS	cation:proton antiporter
1	P4G95_05570	MarR family winged helix-turn-helix transcriptional regulator CDS	MarR family winged helix-turn-helix transcriptional regulator
1	P4G95_06510 and P4G95_06515	paaK and paaJ CDS	phenylacetate-CoA oxygenase/reductase subunit PaaK and phenylacetate-CoA oxygenase subunit PaaJ
1	P4G95_13560	phaR	polyhydroxyalkanoate synthesis repressor PhaR
1	P4G95_13570	acetyl-CoA C-acetyltransferase CDS	acetyl-CoA C-acetyltransferase
1	Between P4G95_15285 and P4G95_15290	Between cupin domain-containing protein CDS and hypothetical protein	
2	P4G95_16325	helix-turn-helix domain-containing protein CDS	helix-turn-helix domain-containing protein
2	P4G95_20810	hypothetical protein CDS	hypothetical protein
3	Between P4G95_29770 and P4G95_29775	Between porin CDS and helix-turn-helix domain-containing protein CDS	

796

797

798 **Table 3.** List of bacterial strains and plasmids used in this work.

Strain or plasmid	Features	Source
Burkholderia cenocepacia K56-2	ET12 lineage cystic fibrosis clinical isolate from Toronto	(61)
Burkholderia cenocepacia F9141525	Cystic fibrosis clinical isolate from Toronto	SickKids, Toronto
Burkholderia cenocepacia F3071909	Cystic fibrosis clinical isolate from Toronto	SickKids, Toronto
Burkholderia cenocepacia G1181568-1	Cystic fibrosis clinical isolate from Toronto	SickKids, Toronto
Burkholderia cenocepacia F4200989-3	Cystic fibrosis clinical isolate from Toronto	SickKids, Toronto
Burkholderia cenocepacia VC14488	Canadian cystic fibrosis isolate	CBCCRRR
Burkholderia cenocepacia VC14543	Canadian cystic fibrosis isolate	CBCCRRR
Burkholderia cenocepacia VC10414	Canadian cystic fibrosis isolate	CBCCRRR
Burkholderia cenocepacia VC14761	Canadian cystic fibrosis isolate	CBCCRRR
Burkholderia cenocepacia 130723	Clinical respiratory isolated collected in Halifax	CANWARD/CARA database
Burkholderia cenocepacia 125007	Clinical respiratory isolated collected in Vancouver	CANWARD/CARA database
Burkholderia contaminans 21NG595759	Canadian cystic fibrosis isolate	H. Adam (Shared Health MB)
Burkholderia contaminans 21NG609698	Canadian cystic fibrosis isolate	H. Adam (Shared Health MB)
Burkholderia dolosa AU6940	Cystic fibrosis clinical isolate	SickKids, Toronto
Burkholderia dolosa AU2167	Cystic fibrosis clinical isolate	SickKids, Toronto
Burkholderia dolosa LM018941	Cystic fibrosis clinical isolate	SickKids, Toronto
Burkholderia dolosa AU0645	Cystic fibrosis clinical isolate	SickKids, Toronto
Burkholderia gladioli VC19233	Canadian cystic fibrosis isolate	CBCCRRR
Burkholderia gladioli VC14812	Canadian cystic fibrosis isolate	CBCCRRR
Burkholderia gladioli 132208	Clinical respiratory isolated collected in Montreal	CANWARD/CARA database

Burkholderia gladioli 113611	Clinical respiratory isolated collected in Saskatoon	CANWARD/CARA database
Burkholderia multivorans 21NH942533	Canadian cystic fibrosis isolate	H. Adam (Shared Health MB)
Burkholderia multivorans 21NJ503211	Canadian cystic fibrosis isolate	H. Adam (Shared Health MB)
Burkholderia multivorans V1120157	Cystic fibrosis clinical isolate	SickKids, Toronto
Burkholderia multivorans LM013010	Cystic fibrosis clinical isolate	SickKids, Toronto
Burkholderia multivorans F9091687	Cystic fibrosis clinical isolate	SickKids, Toronto
Burkholderia multivorans VC19694	Canadian cystic fibrosis isolate	CBCCRRR
Burkholderia multivorans VC15555	Canadian cystic fibrosis isolate	CBCCRRR
Burkholderia multivorans VC9825	Canadian cystic fibrosis isolate	CBCCRRR
Burkholderia multivorans 131077	Clinical respiratory isolated collected in Toronto	CANWARD/CARA database
Burkholderia stagnalis MSMB618	N/A	NAU-PMI
Burkholderia stagnalis MSMB642	N/A	NAU-PMI
Burkholderia vietnamiensis LMG 22486	Wastewater isolate	BCCM
Burkholderia vietnamiensis LMG 10929	Oryza sativa, rhizosphere soil isolate	BCCM
Burkholderia vietnamiensis LMG 16232	Clinical isolate from cystic fibrosis patient	BCCM
Burkholderia vietnamiensis VC11431	Canadian cystic fibrosis isolate	CBCCRRR
Burkholderia vietnamiensis VC18984	Canadian cystic fibrosis isolate	CBCCRRR
Burkholderia vietnamiensis LMG 16232 *lip1*::CAST-Tp	Derived from LMG 16232; Cargo containing Tp^r integrated into triacylglycerol lipase CDS (P4G95_16805)	This study
Burkholderia vietnamiensis LMG 16232 A24 family peptidase CDS:: CAST-Tp	Derived from LMG 16232; Cargo containing Tp^r integrated into A24 family peptidase CDS (P4G95_07805)	This study
Burkholderia vietnamiensis LMG 16232 *otsB*::CAST-Tp	Derived from LMG 16232; Cargo containing Tp^r integrated into *otsB* (P4G95_10885)	This study

Burkholderia vietnamiensis LMG 16232 *gspE*::CAST-Tp	Derived from LMG 16232; Cargo containing Tp^r integrated into *gspE* (P4G95_05530)	This study
Burkholderia vietnamiensis LMG 16232 TetR/AcrR family transcriptional regulator CDS::CAST-Tp	Derived from LMG 16232; Cargo containing Tp^r integrated into TetR/AcrR family transcriptional regulator CDS (P4G95_00865)	This study
E. coli Stbl2	*F- mcrA Δ(mcrBC-hsdRMS-mrr) recA1 endA1lon gyrA96 thi supE44 relA1* λ^- *Δ(lac-proAB)*	Invitrogen
pRBrhaBoutgfp	pSCrhaBoutgfp derivative, ori_{R6K}, *rhaR rhaS* PrhaB e-gfp	(62)
pRK2013	ori_{colE1} RK2 derivative Kan^r mob^+ tra^+	(63)
pDonorTp	pDonor_ShCAST_kanR with modification of Km^R to Tp^R	(24)
pRhaCAST	*Sh-cas12K-tnsBC-tniQ* drives by the rhamnose inducible promoter	(24)
pRhaCAST-3668	Modified from pRhaCAST. crRNA targeting *B. vietnamiensis* LMG 16232 triacylglycerol lipase CDS (P4G95_16805)	This study
pRhaCAST-3952	Modified from pRhaCAST. crRNA targeting *B. vietnamiensis* LMG 16232 A24 family peptidase CDS (P4G95_07805)	This study
pRhaCAST-3956	Modified from pRhaCAST. crRNA targeting *B. vietnamiensis* LMG 16232 *otsB* (P4G95_10885)	This study
pRhaCAST-3996	Modified from pRhaCAST. crRNA targeting *B. vietnamiensis* LMG 16232 *gspE* (P4G95_05530)	This study
pRhaCAST-4000	Modified from pRhaCAST. crRNA targeting *B. vietnamiensis* LMG 16232 TetR/AcrR family transcriptional regulator CDS (P4G95_00865)	This study

Table 4. Primers/templates used in this study

Number	Sequence	Description
Oligonucleotides for Tn-seq		
683	CCGTAGTGAGTTCTTCGTCCGAGCCA CTCGGAGATGTGTATAAGAGACAGT	Tn-seq adapter (top strand)
684	CTGTCTCTTATACACATCTCCGAGTG GCTCGGACGAAGAACTCACTACGG	Tn-seq adapter (bottom strand)

682	CACAAGTGCGGCCGCACTAGTCTAG ATTTAAATTACCGTAGTGAGTTCTTC GTCCGAGCCAC	Tn-seq oligo probe
681	CAAGCAGAAGACGGCATACGAGATT CGCCTTAGTCTCGTGGGCTCGGAGAT GTGTATAAGAGACAG	Illumina Nextera index N701 (Pool 1)
690	AATGATACGGCGACCACCGAGATCT ACACTAGATCGCTCGTCGGCAGCGTC AGATGTGTATAAGAGACAGNNNNAA TCTAGACTAGTGCGGCC	Illumina Nextera index N501 (Pool 1)
718	CAAGCAGAAGACGGCATACGAGATA GGAGTCCGTCTCGTGGGCTCGGAGAT GTGTATAAGAGACAG	Illumina Nextera index N705 (Pool 2)
719	AATGATACGGCGACCACCGAGATCT ACACCTCTCTATTCGTCGGCAGCGTC AGATGTGTATAAGAGACAGNNNNAA TCTAGACTAGTGCGGCC	Illumina Nextera index N502 (Pool 2)
Oligonucleotides for cloning crRNA into pRhaCAST (crRNA is in bold, *sapI* restriction site is in italics)		
3392	ACTAACGGCTCTTCGAG	Reverse primer to amplify single stranded nucleotide template containing the crRNA
3421	CATTGGCTCTTCGAAAG	Forward primer to amplify single stranded nucleotide template containing the crRNA
3668	CATT*GGCTCTTC*GAAAG**ATCCTCGTG CACGGCCTTACCGGC**GGCTC*GAAGA GC*CGTTAGT	Targeting triacylglycerol lipase CDS (P4G95_16805) of LMG 16232
3952	CATT*GGCTCTTC*GAAAG**GTGATCGG TCTGTGCGTCGGCAGC**GGCTC*GAAG AGC*CGTTAGT	Targeting A24 family peptidase CDS (P4G95_07805) of LMG 16232
3956	CATT*GGCTCTTC*GAAAG**CCTGACCG ATACCGCGTTCTTTTT**GGCTC*GAAG AGC*CGTTAGT	Targeting *otsB* (P4G95_10885) of LMG 16232
3996	CATT*GGCTCTTC*GAAAG**TGCAAGGA AGAGCGACACGAGGAC**GGCTC*GAA GAGC*CGTTAGT	Targeting *gspE* (P4G95_05530) of LMG 16232
4000	CATT*GGCTCTTC*GAAAG**CCACCATCG ACGAGACCTGGTCGT**GGCTC*GAAGA GC*CGTTAGT	Targeting TetR/AcrR family transcriptional regulator CDS (P4G95_00865) of LMG 16232
Oligonucleotides for colony PCR to verify genomic insertion		
3001	GGTGGGTTGAAAGCAAGTCC	left end of the cargo insertion
3670	CTATCCGGTCATCCTCGTGC	Colony PCR for triacylglycerol lipase CDS (P4G95_16805) of LMG 16232
3953	GTGATCGGTCTGTGCGTCG	Colony PCR for A24 family peptidase CDS (P4G95_07805) of LMG 16232
3957	CTGACCGATACCGCGTTCTT	Colony PCR for *otsB* (P4G95_10885) of LMG 16232

3997	GCAAGGAAGAGCGACACGAG	Colony PCR for *gspE* (P4G95_05530) of LMG 16232
4001	CCACCATCGACGAGACCTG	Colony PCR for TetR/AcrR family transcriptional regulator CDS (P4G95_00865) of LMG 16232

801